TYPE 1 DIABETES

Immune responses to gut bacteria associated with time to diagnosis and clinical response to T cell–directed therapy for type 1 diabetes prevention

Quin Yuhui Xie[1,2], Sean Oh[2], Anthony Wong[2], Christopher Yau[2,3], Kevan C. Herold[4,5], Jayne S. Danska[1,2,3]*

Immune-targeted therapies have efficacy for treatment of autoinflammatory diseases. For example, treatment with the T cell–specific anti-CD3 antibody teplizumab delayed disease onset in participants at high risk for type 1 diabetes (T1D) in the TrialNet 10 (TN-10) trial. However, heterogeneity in therapeutic responses in TN-10 and other immunotherapy trials identifies gaps in understanding disease progression and treatment responses. The intestinal microbiome is a potential source of biomarkers associated with future T1D diagnosis and responses to immunotherapy. We previously reported that antibody responses to gut commensal bacteria were associated with T1D diagnosis, suggesting that certain antimicrobial immune responses may help predict disease onset. Here, we investigated anticommensal antibody (ACAb) responses against a panel of taxonomically diverse intestinal bacteria species in sera from TN-10 participants before and after teplizumab or placebo treatment. We identified IgG2 responses to three species that were associated with time to T1D diagnosis and with teplizumab treatment responses that delayed disease onset. These antibody responses link human intestinal bacteria with T1D progression, adding predictive value to known T1D risk factors. ACAb analysis provides a new approach to elucidate heterogeneity in responses to immunotherapy and identify individuals who may benefit from teplizumab, recently approved by the U.S. Food and Drug Administration for delaying T1D onset.

INTRODUCTION

Advances in understanding the pathologic mechanisms of autoimmune and inflammatory diseases have facilitated the clinical advancement of immunomodulatory drugs (*1*–*10*). Antibodies and fusion proteins targeting CD20 on B lymphocytes and proinflammatory cytokines such as tumor necrosis factor (TNF), interleukin-17 (IL-17), and IL-23 have shown efficacy in the treatment of relapse-remitting multiple sclerosis, plaque psoriasis, and Crohn's disease (*1*–*5*). A recurrent observation in these settings is variation in treatment responses. Given the resource demands of clinical trials of immunomodulatory drugs, heterogeneity in patient responses propels efforts to identify biomarkers reflective of either the pathophysiology targeted by the treatment or a subset of patients most likely to respond within the trial period (*2*, *3*, *7*, *9*, *11*).

Type 1 diabetes (T1D) is mediated by T cells that destroy insulin-secreting β cells in the pancreatic islets (*12*–*14*). Decades of research have identified *HLA-DR* haplotypes and the appearance of islet autoantibodies (IABs) in the blood as biomarkers of disease risk (*15*–*17*). However, the mechanisms underlying heterogeneity in T1D progression, including the contributions of genetic risk loci, the number and antigen specificity of IAB, the age of IAB appearance, and time to T1D onset, have not been fully elucidated. The search for biomarkers predictive of disease onset is particularly relevant in T1D because the intervention window for preserving β cell function is limited and intensive glucose control initiated early after disease onset does not preserve β cell function (*18*).

The T cell–specific anti-CD3 monoclonal antibody teplizumab was tested in patients with recent-onset T1D, where it preserved residual insulin production (*19*). Although the mechanism of effect is not fully elucidated, teplizumab treatment promotes $CD8^+$ T cells to adopt an exhausted state that may reduce activity against β cells (*20*–*23*). In a humanized mouse model, teplizumab resulted in T cell migration to the intestine, resulting in increased expression of immunomodulatory cytokines and suggesting that exposure to the gut mucosal environment contributed to improved β cell tolerance (*24*). A recent T1D prevention trial [TrialNet (TN-10)] enrolled prediabetic individuals with a family history of T1D, presence of ≥2 IABs, and dysglycemia (*10*) who were randomized to a 14-day course of treatment with teplizumab or a placebo. TN-10 met the primary outcome, delay in diabetes diagnosis by a median of 32.5 months (*10*, *25*) and improved β cell function (*25*, *26*). Increased frequencies of T cells with an exhausted phenotype were associated with these clinical effects (*20*–*23*). These results prompted the recent approval of teplizumab to delay T1D onset by the U.S. Food and Drug Administration (FDA) (*27*).

The TN-10 trial provided the first demonstration that a T cell–directed therapy could delay onset of an autoimmune disease; however, participant responses were heterogeneous. Better treatment outcomes were associated with *HLA* class II genotype, presence of *HLA-DR4* and absence of *HLA-DR3*, and presence of residual insulin production (C-peptide responses) (*10*). Remaining critical gaps in knowledge include understanding the basis of heterogeneity in patient teplizumab responses and expanding the suite of biomarkers to better identify prediabetic and new-onset participants most likely to benefit from treatment.

[1]Department of Medical Biophysics, University of Toronto, Toronto, Ontario M5T2S8, Canada. [2]Genetics and Genome Biology, Hospital for Sick Children, Toronto, Ontario M5G1X8, Canada. [3]Department of Immunology, University of Toronto, Toronto, Ontario M5T2S8, Canada. [4]Department of Immunobiology, Yale University, New Haven, CT 06520, USA. [5]Department of Internal Medicine, Yale University, New Haven, CT 06520, USA.
*Corresponding author. Email: jayne.danska@sickkids.ca

Previously, we reported identification of serum antibody responses to live, cultured gut commensal bacteria [anticommensal antibodies (ACAbs] in an observational study of relatives of persons with T1D (*28*). Several of the identified ACAb reactivities displayed *HLA-DR* dependence and were associated with the presence of IAB before diabetes development. Given these findings, we reasoned that the patterns of ACAbs might reveal associations with beneficial teplizumab responses in the TN-10 participants. Extensive studies have sought to identify changes in composition of the gut microbiome in young children at risk for T1D, after islet antibody seroconversion, and at the onset of clinical diabetes (*29*). Here, we tested the hypothesis that immune reactivities to gut bacteria are associated with progression to T1D and with treatment responses. We characterized ACAb responses in TN-10 participants before and after treatment with teplizumab or placebo and analyzed these results together with the available clinical data. We report that antibody responses to specific intestinal bacteria were associated with time to T1D diagnosis and with teplizumab effects in prediabetic TN-10 trial participants, thus linking immune detection of intestinal microbes with progression and prevention of T1D.

RESULTS

Teplizumab treatment does not alter ACAb or IAB responses

Teplizumab binds to a conserved epitope on the CD3ε component of the T cell antigen receptor. Because T cells provide signals critical to generating many B cell responses, we first tested the stability of antibody responses in the sera of available TN-10 trial participants ($n = 63$). All individuals in the current study had one serum sample taken before and at least one serum sample taken after randomization into teplizumab or placebo treatment arms (fig. S1). The median age was 14 (8 to 49), and age ($P = 0.73$), sex ($P = 0.80$), and *HLA-DR* haplotypes (*HLA-DR3* $P = 1$, *HLA-DR4* $P = 0.78$) were not significantly different across treatment arms (Table 1). Previous studies demonstrated that teplizumab delays T1D diagnosis by a median of 32.5 months in the entire study cohort (*10*, *25*). In the subset of participants whose samples were available for this study, the effect of teplizumab on delaying T1D diagnosis remained significant ($P = 0.046$), with a median time to T1D of 30.6 months in the placebo versus 61.1 months in the teplizumab group (fig. S2) (*30*).

Our study was designed to characterize anticommensal responses of isotypes immunoglobulin G1 (IgG1), IgG2, and IgA in serum samples ($n = 228$) from trial participants either before or up to 18 months after randomization into treatment arms (Fig. 1A). We measured the abundance of ACAb isotypes against a panel of 31 bacterial strains representing 15 common species, distributed across the four major phyla found in healthy human gut microbiota (Fig. 1B and table S1). First, we examined all ACAb responses in serum samples isolated at baseline and up to 18 months after randomization. Responses to these bacterial targets were stable across time in both treatment groups for each of the three isotypes (fig. S3, A to C). We also quantified total serum IgG1, IgG2, and IgA antibody concentrations in participant samples displaying the well-known higher serum abundance of IgG1 (Fig. 2A) and observed no significant changes across time (12 months $P = 0.13$, 24 months $P = 0.05$, 36 months $P = 0.16$) or treatment arms ($P = 0.16$) compared to baseline (Fig. 2B). To examine relationships between responses across isotypes, we performed principal components analysis (PCA) on all ACAb responses at baseline (fig. S3D) and at 6-month (fig. S3E) time points. The first two PCs (36% of the variance) reflected differences between IgG1 compared with IgG2 and IgA responses that displayed more similar patterns. IgG1 is vital for antiviral responses, whereas IgG2 primarily recognizes bacterial capsular polysaccharides and IgA binds to bacterial surface proteins, many associated with major human pathogens. These PCs may reflect the distinct effector outcomes of these isotypes: Whereas IgG1 responses are predominantly proinflammatory, IgG2 and IgA responses contribute to maintenance of mucosal and systemic homeostasis *(31)*.

The TN-10 participants were assessed for IABs against four antigens [glutamic acid decarboxylase 65 antibodies (GADA), insulinoma associated protein 2 antibodies (IA2A), micro-insulin autoantibodies (mIAA), and zinc transporter 8 antibodies (ZnT8A)]. Consistent positivity for ≥2 of these IAB was an inclusion criterion for the trial (*10*). IAB titers were collected from randomization until T1D diagnosis. These IAB specificities did not differ between participants in the two treatment groups at baseline (Table 1) or at any time after randomization (Fig. 2C). Quantitatively, IAB displayed stable abundances and specificities across the observation period (Fig. 2D), and there were no significant differences in the trajectories of ACAb responses over time in either treatment arm (fig. S3, A to C). Thus, the temporal stability of both IAB and

Table 1. TN-10 participants were randomized across treatment arms in terms of baseline characteristics. The difference in distribution of continuous variables (such as age, BMI, and C-peptide) across the two treatment arms was tested by Welch two-sample *t* test. The difference in distribution of discrete variables across treatment arms was tested by Fisher's exact test. No significant difference across treatment arms was found.

Baseline characteristics	Teplizumab (*n* = 41)	Placebo (*n* = 22)
Age		
Median (IQR)	14 (11–21)	14 (11–15.8)
Range	8–49	8–45
Male [*n* (%)]	22 (54)	11 (50)
BMI [median (IQR)]	20.0 (17.3–25.5)	21.7 (18.4–24.8)
C-peptide [median (IQR)]	1.8 (1.5–2.1)	2.1 (1.6–2.7)
HLA-DR carriage [*n* (%)]		
HLA-DR3	18 (45)	10 (42)
HLA-DR4	27 (66)	14 (64)
Islet autoantibody positivity [*n* (%)]		
Glutamic acid decarboxylase 65 antibodies (GADA)	5 (12)	3 (14)
Micro-insulin autoantibodies (mIAA)	17 (41)	11 (50)
Insulinoma-associated protein 2 antibodies (IA2A)	15 (36)	4 (18)
Zinc transporter 8 antibodies (ZnT8A)	11 (27)	3 (14)

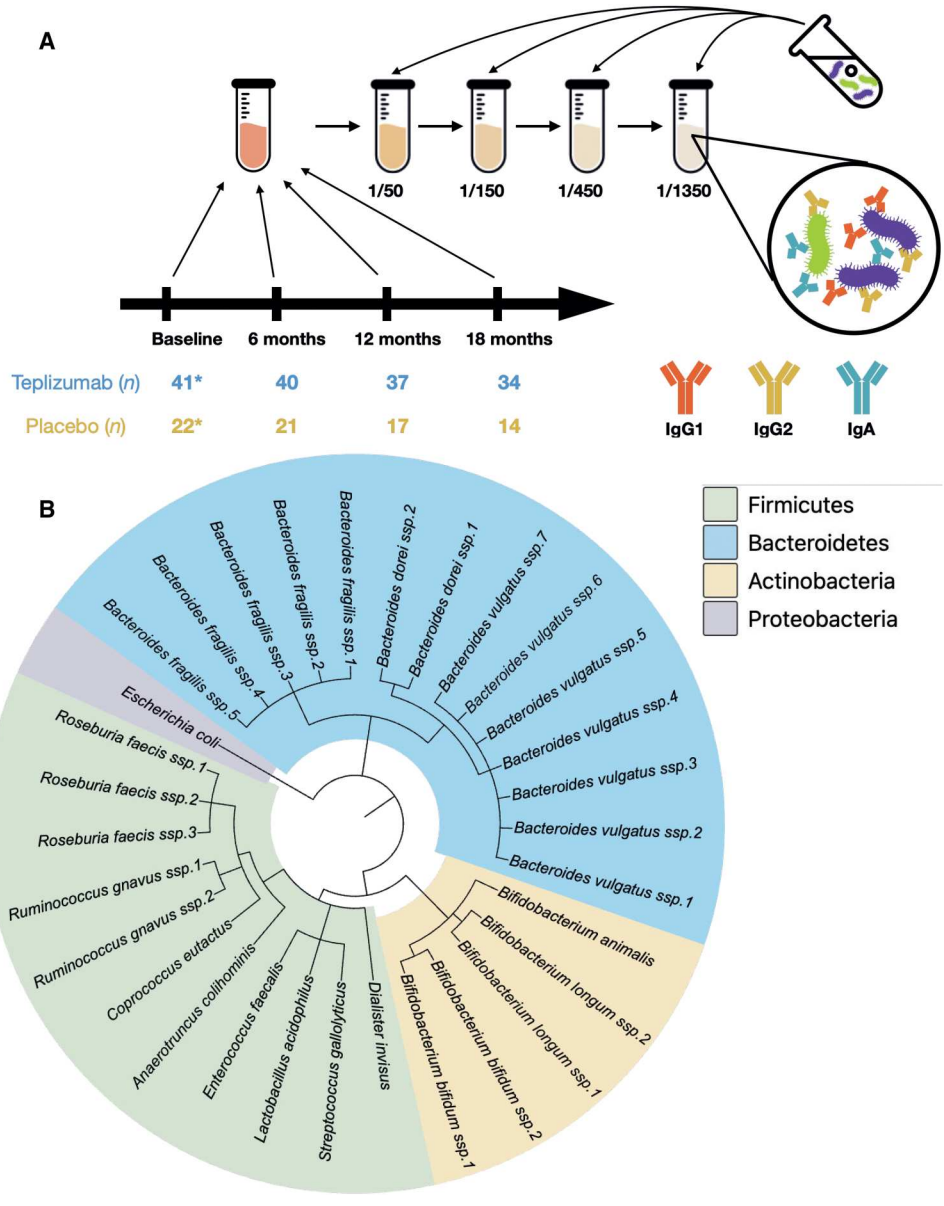

Fig. 1. Experimental design for ACAb response characterization in the TN-10 cohort. (**A**) Simple schematic of an ACAb experiment for one sample. Four serial dilutions of a serum sample were incubated with two bacteria species stained with amine-reactive dyes to quantify serum antibodies bound to bacterial surface antigens. *One duplicate sample in each treatment arm is for quality control and not included in the sample count. (**B**) Phylogenetic tree of bacterial strains used in ACAb assays. Multiple strains for a species were used to better represent within-species heterogeneity and maximize antigenic diversity. Plot generated by Interactive Tree Of Life (*88*).

ACAb profiles suggested that antibody responses were not altered by teplizumab treatment.

Association of ACAb responses with time to T1D diagnosis and treatment responses

Given the overall stability of both ACAb and IAB measures in both teplizumab- and placebo-treated groups, we asked whether any of the participants' ACAb responses were associated with the primary clinical endpoint, diabetes diagnosis. We performed landmark analysis to eliminate any potential immortal time bias resulting from use of response (T1D diagnosis) as a predictor (*32*–*35*). Forty-five days, after which the transient effects of teplizumab treatment on lymphocyte counts returned to baseline, was selected as the landmark (*10*). Because the earliest time to T1D diagnosis was 95 days, landmark analysis did not require removal of any of the participants. We then used boosted Cox models (*36*) to identify baseline variables and ACAb responses associated with T1D diagnosis and used linear Cox models (*37*) to estimate their effects on time to diagnosis. We identified IgG2 responses to three bacterial species at baseline and at 6 months that were associated with time to T1D diagnosis. ACAb profiles and statistical significance of these associations are presented below for the actinobacteria *Bifidobacterium longum* as well as the firmicutes *Enterococcus faecalis* and *Dialister invisus*.

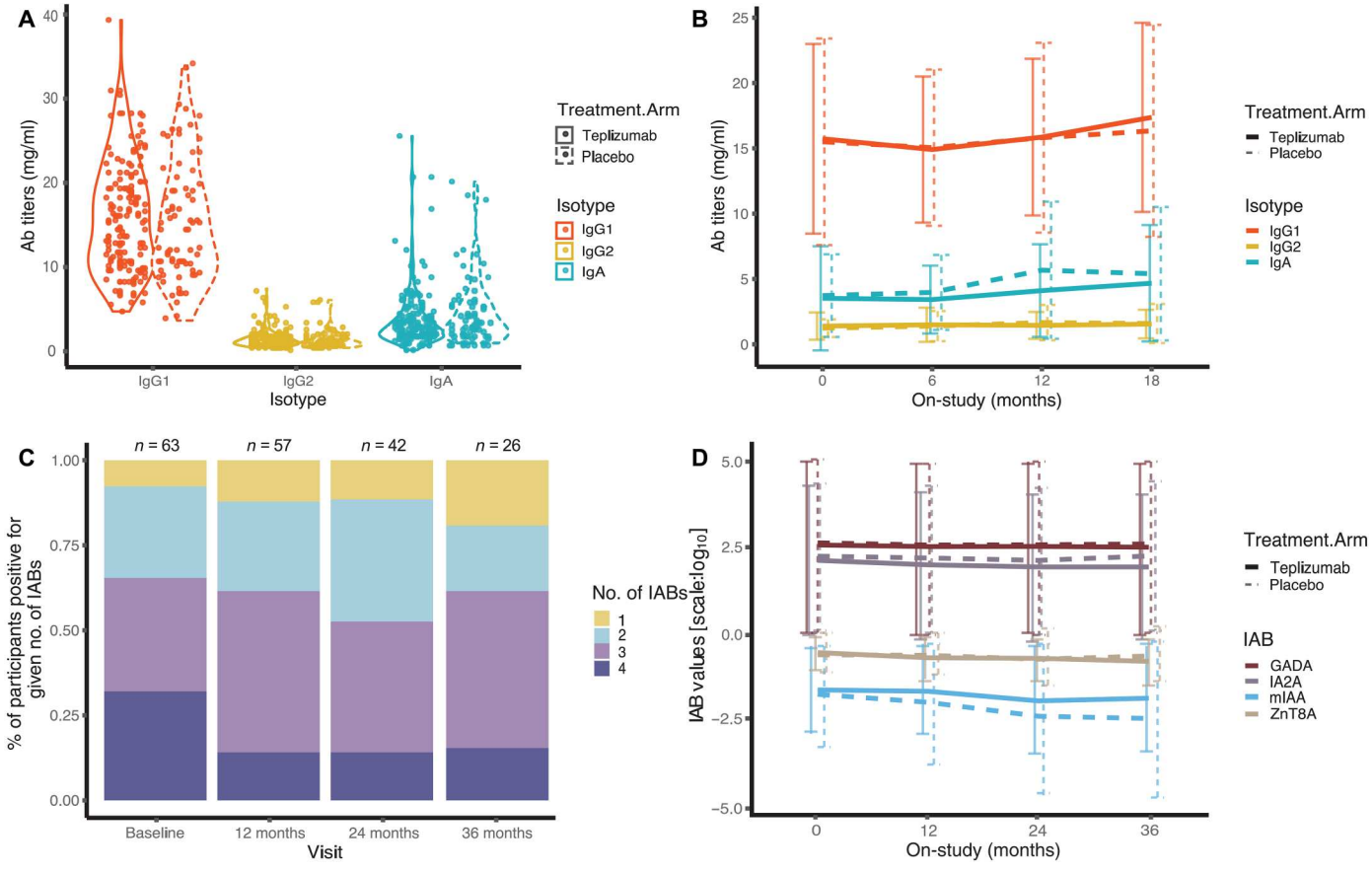

Fig. 2. Teplizumab treatment does not change the total antibody isotype titers or the magnitude of antibody responses to four defined islet antigens. (**A**) Titers of total IgG1, IgG2, and IgA antibodies in teplizumab versus placebo groups aggregating across time points measured by ELISA (IgG1, red; IgG2, yellow; IgA, blue; teplizumab, solid line; placebo, dashed line). (**B**) Trajectories of total IgG1, IgG2, and IgA antibodies over time. No significant difference across treatment arms or time points. (**C**) Percentage of participants positive for one, two, three, or four IABs at single time points before or after randomization across treatment arms. No significant difference in distribution across treatment arms or time points. (**D**) Trajectories of GADA, IA2A, mIAA, and ZnT8A over time (GADA, red; IA2A, purple; mIAA, blue; ZnT8A, brown; teplizumab, solid line; placebo, dashed line). The *y* axis was $\log_{10}$-transformed to display IAB titers with different scales. No significant difference in IAB abundance across treatment arms or time points. Vertical bars are SDs within treatment arms at a single time point. Color palette from ghibli (v0.3.3) (*89*).

The *B. longum*–IgG2 response was bimodal when aggregated across all time points in this cohort (Fig. 3A). When segregated by time point, the *B. longum*–IgG2 response remained bimodal at baseline (Fig. 3B) and at 6 months (Fig. 3C), the closest time point for which samples were available after randomization. We found that the probability of progressing to T1D diagnosis positively correlated with *B. longum*–IgG2 responses at baseline (Cox model, *B. longum*–IgG2 $P = 0.011$, treatment arm $P = 0.031$). We selected the trough between the two response modes to dichotomize the participants into high and low *B. longum*–IgG2 responders for Kaplan-Meier analysis (Fig. 3, D to F). The teplizumab treatment effect in the anti–*B. longum*–IgG2 subgroup was greater in those with high baseline titers (Fig. 3E) compared with those with low titers (Fig. 3D). When comparing all four strata (placebo, treatment, high, and low baseline titers), the highest risk of T1D onset was seen in the placebo-treated, high baseline *B. longum*–IgG2 response subgroup (Fig. 3F). In contrast, the teplizumab-treated, high baseline *B. longum*–IgG2 response subgroup displayed reduced risk (pairwise log-rank $P = 0.0221$, Benjamini-Hochberg–adjusted), suggesting that *B. longum*–IgG2 responses at baseline were predictive of responders to teplizumab treatment. Because ACAb responses were stable over time (fig. S3), we performed regression analyses of the 6-month *B. longum*–IgG2 responses. Six months after randomization, *B. longum*–IgG2 response remained associated with progression to T1D diagnosis (Cox model, *B. longum*–IgG2 $P = 0.007$, treatment arm $P = 0.031$) in the entire cohort. Like our observations at baseline, a less evident teplizumab treatment response was seen for participants in the lower *B. longum*–IgG2 titer subgroup (Fig. 3G) compared with the higher *B. longum*–IgG2 titer subgroup at 6 months (Fig. 3H). Thus, higher *B. longum*–IgG2 responses present at baseline and at 6 months after randomization were associated with greater teplizumab treatment effect.

In contrast to *B. longum*–IgG2, responses to *E. faecalis*–IgG2 displayed a roughly normal distribution across all time points (Fig. 4A) and at single time points (baseline; Fig. 4B; 6 months; Fig. 4C). We performed regression analyses on *E. faecalis*–IgG2 responses at baseline (Fig. 4, D and E) and at 6 months (Fig. 4, F and G) using the median (all samples across all time points) to define high versus low responses. *E. faecalis*–IgG2 responses at both time points were associated with time to T1D diagnosis (Cox model, baseline *E.*

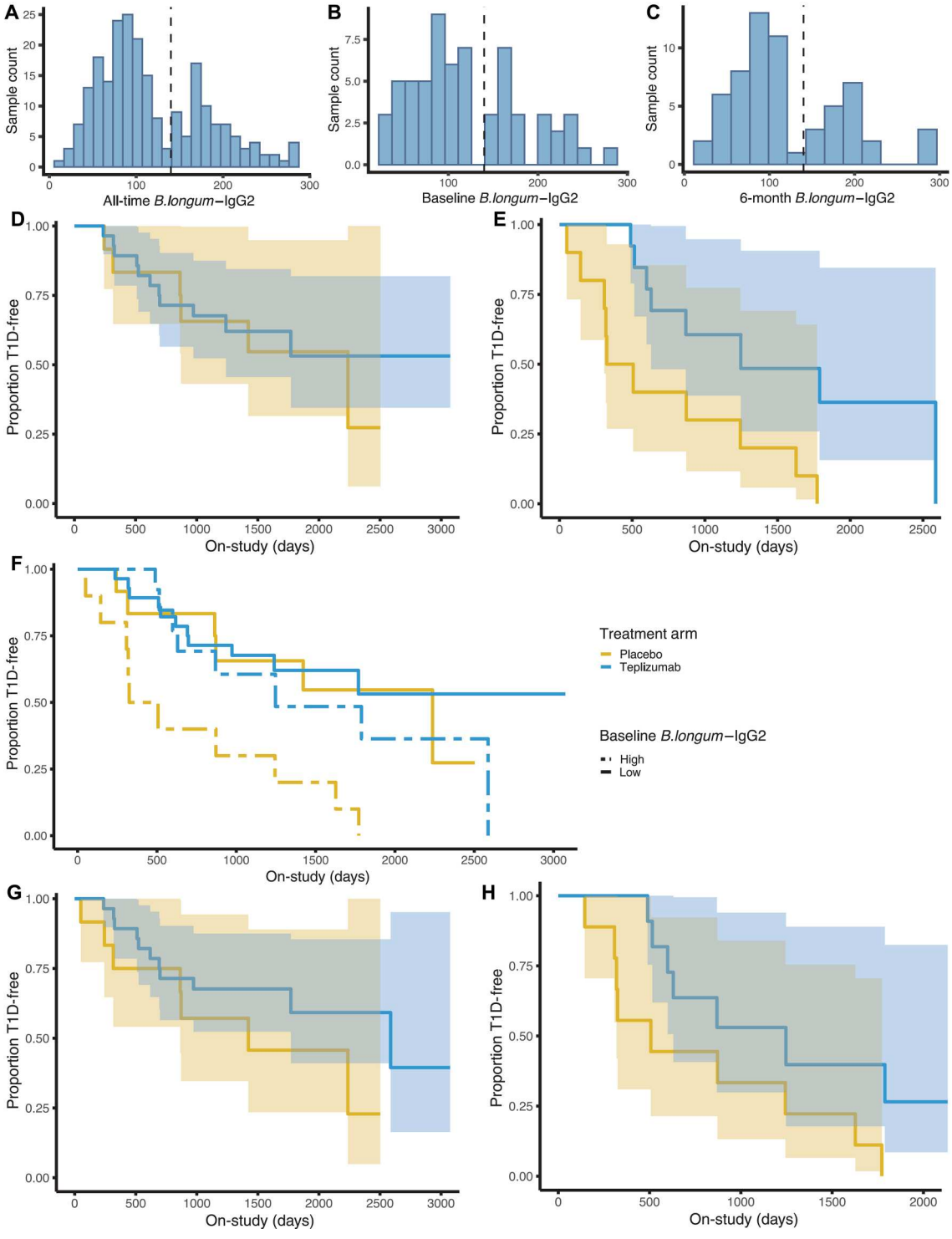

Fig. 3. Baseline and 6-month *B. longum*–IgG2 response indices are associated with time to T1D diagnosis and teplizumab treatment effect. Distribution of *B. longum*–IgG2 response indices across time points (**A**), at baseline (**B**), and at 6 months (**C**). The vertical dashed line ($x = 140$) marks the trough between the two modes and the cutoff for high and low subgroups. Proportion of participants remaining T1D-free in each treatment arm (teplizumab, blue; placebo, yellow) separately in low (**D**) and high (**E**) *B. longum*–IgG2 response subgroups at baseline [Wald test $P = 0.011$, hazard ratio (HR) = 1.007] and together (**F**) (low, solid line, $n = 12$ placebo, $n = 28$ teplizumab; high, dashed line, $n = 10$ placebo, $n = 13$ teplizumab; log-rank $P = 0.0011$). Proportion of participants remaining T1D-free in each treatment arm in low (**G**) ($n = 12$ placebo, $n = 28$ teplizumab) and high (**H**) ($n = 9$ placebo, $n = 11$ teplizumab) *B. longum*–IgG2 response subgroups at 6 months (Wald test $P = 0.007$, HR = 1.008). HRs estimated by multivariate Cox PH adjusting for age, sex, BMI, treatment arm, and *HLA-DR*.

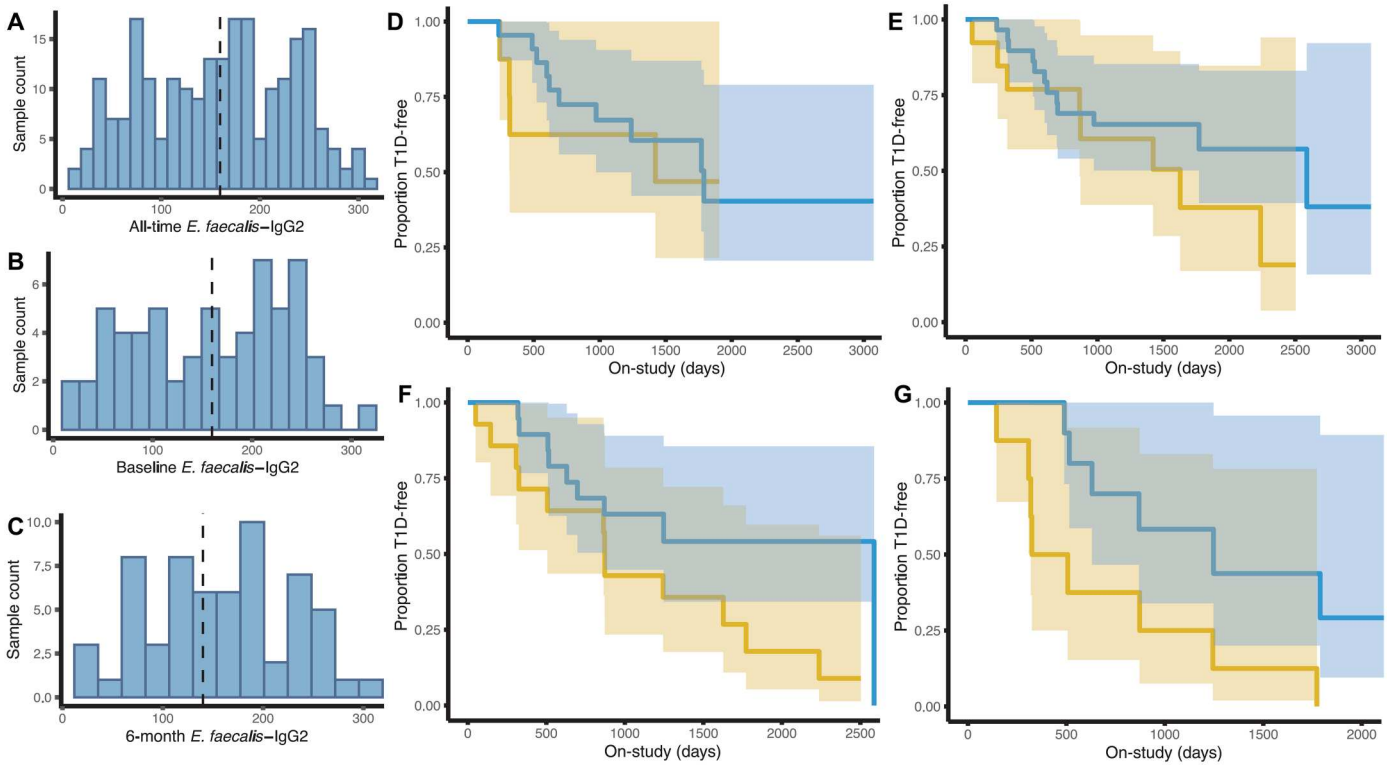

Fig. 4. Baseline and 6-month *E. faecalis*–IgG2 response indices are associated with time to T1D diagnosis. Distribution of *E. faecalis*–IgG2 response indices across time points (**A**), at baseline (**B**), and at 6 months (**C**). The vertical dashed line (x = 159.61) marks the median *E. faecalis*–IgG2 response indices of all samples across time points and the cutoff for high and low subgroups. Proportion of participants remaining T1D-free in each treatment arm (teplizumab, blue; placebo, yellow) in low (**D**) (n = 8 placebo, n = 22 teplizumab) and high (**E**) (n = 14 placebo, n = 19 teplizumab) baseline *E. faecalis*–IgG2 response subgroups (P = 0.002, HR = 1.008). Proportion of participants remaining T1D-free in each treatment arm in low (**F**) (n = 13 in placebo, n = 29 in teplizumab) and high (**G**) (n = 8 in placebo, n = 10 in teplizumab) 6-month *E. faecalis*–IgG2 response subgroups (P = 0.0009, HR = 1.009). HRs estimated by multivariate Cox PH adjusting for age, sex, BMI, treatment arm, and *HLA-DR*.

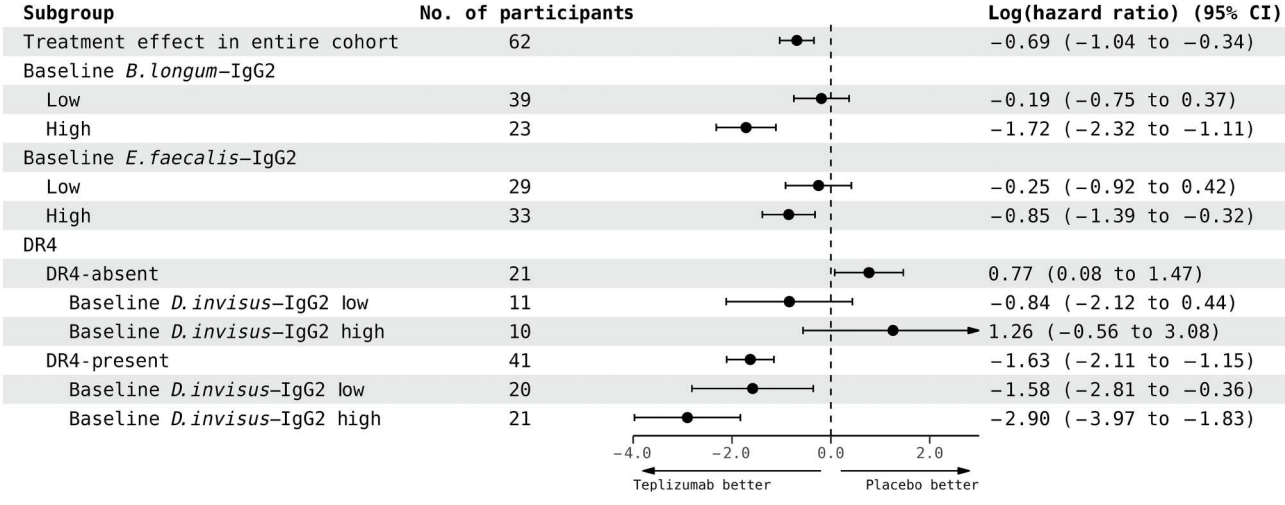

Fig. 5. Responses to teplizumab are associated with baseline IgG2 responses to selected gut bacteria. Log HRs and 95% CIs for T1D diagnosis in the teplizumab group compared with the placebo group for baseline IgG2 response–stratified subgroups. Treatment effect was better in individuals with high baseline *B. longum*–IgG2 and *E. faecalis*–IgG2 responses and, within the DR4-present group, *D. invisus*–IgG2 responses. Multivariate Cox PH models were adjusted for age, sex, BMI, and *HLA-DR*, but not for multiple testing. Plot generated using Forester (v0.2.0) (*90*).

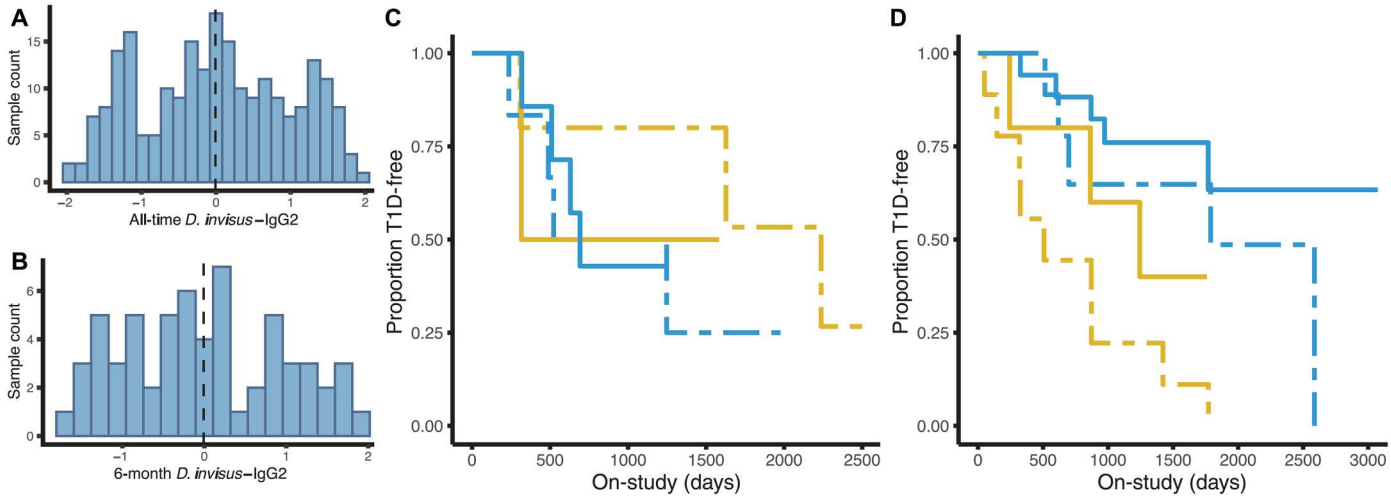

Fig. 6. Six-month *D. invisus*–IgG2 response indices interact with *HLA-DR4* in association with time to T1D. Normalized distribution of *D. invisus*–IgG2 response indices across all time points (**A**) and at the 6-month time point (**B**). The vertical dashed line ($x = -0.009$) marks the median *D. invisus*–IgG2 response indices of all samples across time points and the cutoff for high and low 6-month *D. invisus*–IgG2 response subgroups. Proportion of participants remaining T1D-free in each treatment arm (teplizumab, blue; placebo, yellow) in low (solid line) and high (dashed line) *D. invisus*–IgG2 response subgroups at the 6-month time point in *HLA-DR4*$^-$ (**C**) ($n = 5$ high, placebo; $n = 6$ high, teplizumab; $n = 2$ low, placebo; $n = 7$ low, teplizumab) and *HLA-DR4*$^+$ (**D**) ($n = 9$ high, placebo; $n = 9$ high, teplizumab; $n = 5$ low, placebo; $n = 17$ low, teplizumab) subgroups. Interaction term between 6-month *D. invisus*–IgG2 and *HLA-DR4*, $P = 0.001 < 0.0012$, the adjusted cutoff based on effective number of independent tests (*80*), HR = 3.97 by multivariate Cox PH regression adjusting for age, sex, BMI, treatment arm, *HLA-DR*, and baseline *D. invisus*–IgG2.

faecalis–IgG2 $P = 0.003$, treatment arm $P = 0.023$; 6-month *E. faecalis*–IgG2 $P = 0.0009$, treatment arm $P = 0.033$). At both time points, the teplizumab treatment effect was more evident in the high *E. faecalis*–IgG2 response (baseline, Fig. 4E; 6 months, Fig. 4G) compared with the low response subgroup (baseline, Fig. 4D; 6 months, Fig. 4F). Thus, as observed for *B. longum*–IgG2 responses, greater responses to *E. faecalis* were associated with greater treatment effect.

C-peptide, a moiety cleaved from proinsulin before its co-secretion, is a well-established clinical marker for β cell function, where its decline represents T1D progression (*38*, *39*). We compared the performance of the *E. faecalis* and *B. longum*–IgG2 responses to C-peptide as predictors of time to T1D diagnosis and for their association with teplizumab treatment effect. When aggregated across time (fig. S4A), as well as at single time points (baseline, fig. S4B; 6 months, fig. S4C), the distributions of C-peptide values were asymmetrical. Our analysis of reported C-peptide values for these participants (*10*) showed that they were associated with time to T1D diagnosis at baseline (fig. S4, D and E) and at 6-month (fig. S4, F and G) time points (Cox model, baseline C-peptide $P = 0.022$, treatment arm $P = 0.0094$; 6-month C-peptide $P = 0.044$, treatment arm $P = 0.0456$). The subgroup with lower-than-median baseline C-peptide values (fig. S4D) displayed a greater treatment response compared with the subgroup with higher-than-median baseline C-peptide (fig. S4E). *E. faecalis*– and *B. longum*–IgG2 responses displayed equally robust associations with time to T1D diagnosis compared to C-peptide. These results suggested that these ACAb responses may help to identify individuals at greater risk for T1D diagnosis.

The analyses revealed associations of ACAb responses with time to T1D diagnosis in the TN-10 cohort adjusted for treatment, age, sex, body mass index (BMI), and *HLA-DR* haplotype. Next, we asked whether ACAb responses were associated with the impact of treatment effect separable from association to time to T1D diagnosis, an outcome that was modified by the treatment. We therefore examined the effect of teplizumab treatment in subgroups stratified by baseline *B. longum*– and *E. faecalis*–IgG2 responses using the cutoffs chosen for the Kaplan-Meier analyses (Fig. 5). We found that a high *B. longum*–IgG2 response at baseline was associated with a more robust teplizumab response [hazard ratio, HR (95% confidence interval, CI): high 0.18 (0.10 to 0.33); low 0.83 (0.47 to 1.44)]. In addition, there was a tendency toward better teplizumab responses in the high baseline *E. faecalis*–IgG2 response subgroup [HR (95% CI): high 0.43 (0.25 to 0.73); low 0.78 (0.40 to 1.52)]. These results suggested that baseline ACAb responses may help to identify individuals likely to respond to teplizumab.

HLA-dependent association of ACAb responses to time to T1D and treatment responses

HLA class II haplotypes, particularly the *DR3* and *DR4* variants in populations of European origin, account for most of the T1D genetic risk and together with family history of T1D are effective screening criteria to identify at-risk individuals (*40*–*43*). In the TN-10 trial, treatment response heterogeneity was reported, with *HLA-DR4* carriage associated with better treatment effects (*10*). We examined an observational study of high-risk, prediabetic participants and observed ACAb responses associated with later T1D diagnosis that displayed *HLA-DR* dependence (*27*). Given the importance of HLA class II molecules in the formation of T cell–dependent antibodies (*31*), we asked whether *HLA-DR* haplotypes influenced immune responses to gut bacteria in the TN-10 participants. Here, we investigated ACAb responses 6 months after randomization that displayed *HLA-DR4* associations with time to T1D diagnosis. *D. invisus* is a common gut microbe that has been previously evaluated in studies of T1D risk using fecal samples from pediatric cohorts (*44*, *45*). We found that *D. invisus*–IgG2 responses

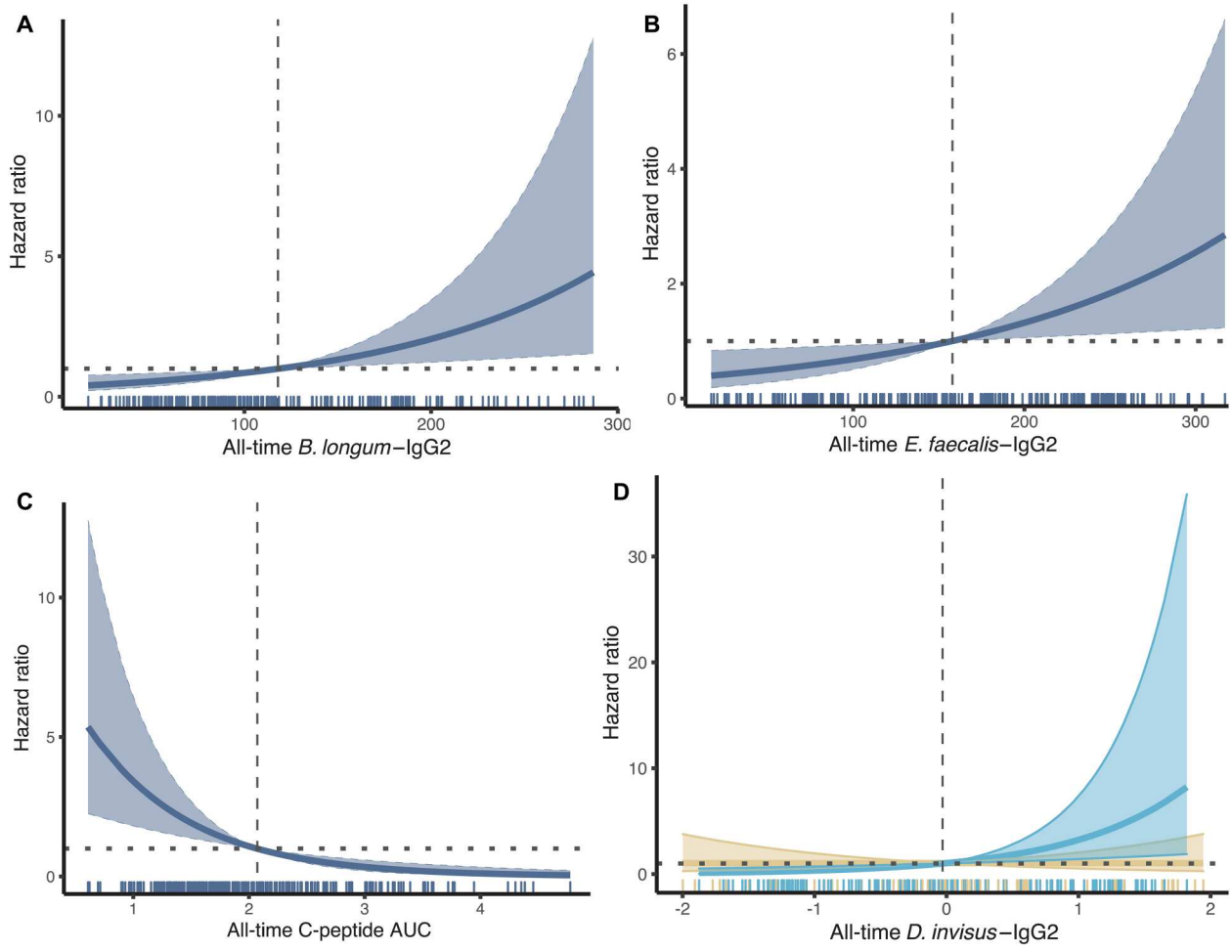

Fig. 7. ACAb responses across time points and C-peptide values are associated with T1D progression. HR of progressing to T1D diagnosis as a function of *B. longum*–IgG2 responses (**A**) (P = 0.006, HR = 1.009), *E. faecalis*–IgG2 responses (**B**) (P = 0.015, HR = 1.006), C-peptide value (**C**) (P = 0.0001, HR = 0.32), and normalized *D. invisus*–IgG2 responses, stratified by *HLA-DR4* (**D**) (*HLA-DR4*$^+$, blue; *HLA-DR4*$^-$, yellow; *D. invisus*–IgG2 P = 0.02, HR = 0.46; *D. invisus*–IgG2–*HLA-DR4* interaction P = 0.005, HR = 3.12) aggregating across time points. HR estimated by time-dependent Cox model adjusting for age, sex, BMI, treatment arm, and *HLA-DR*. Horizontal dashed lines are placed at HR = 1, indicating no change in risk of progressing to T1D diagnosis. Vertical dashed lines are placed at the mean ACAb responses (*B. longum*–IgG2, x = 118.05; *E. faecalis*–IgG2, x = 158.02; normalized *D. invisus*–IgG2, x = 0) or C-peptide value (x = 2.09) of the cohort.

interacted with *HLA-DR4* in association with time to T1D onset (Cox model, *D. invisus*–IgG2–*HLA-DR4* interaction P = 0.001, treatment arm P = 0.021). We transformed *D. invisus*–IgG2 responses across all time points to a standard normal distribution for regression analyses (Fig. 6, A and B). The median *D. invisus*–IgG2 response was used as the cutoff to define high versus low 6-month response subgroups. When segregating participants by *HLA-DR4* genotype, we found that associations of *D. invisus*–IgG2 responses either with time to T1D diagnosis or with treatment effect were absent in the *HLA-DR4*$^-$ subgroup (Fig. 6C). In contrast, *HLA-DR4*$^+$ individuals (Fig. 6D) with higher 6-month *D. invisus*–IgG2 responses (dashed line) were at greater risk for progressing to T1D than the subgroup with lower 6-month *D. invisus*–IgG2 responses (solid line). Moreover, teplizumab treatment of *HLA-DR4*$^+$ individuals independently delayed T1D onset in both high and low *D. invisus*–IgG2 response subgroups compared with placebo treatment (Fig. 6D, blue and yellow lines, respectively).

To examine the predictive value of *D. invisus*–IgG2 responses for response to teplizumab, we compared treatment effect in subgroups stratified by *HLA-DR4* genotype and baseline *D. invisus*–IgG2 responses. Building on evidence that *HLA-DR4* presence is associated with better teplizumab response, we observed that in *HLA-DR4*–absent participants, higher baseline *D. invisus*–IgG2 response was associated with greater probability of progression to T1D diagnosis despite teplizumab treatment [HR (95% CI): high 3.51 (0.57 to 21.67); low 0.43 (0.12 to 1.55)]. In contrast, higher baseline *D. invisus*–IgG2 responses in *HLA-DR4*–present participants were associated with better outcome [HR (95% CI): high 0.05 (0.02 to 0.16); low 0.21 (0.06 to 0.70)]. Collectively, these results suggested that *D. invisus*–IgG2 responses displayed an interaction with *HLA-DR4* haplotype in their association with T1D progression and with teplizumab treatment response. Specifically, *HLA-DR4*$^+$ individuals with high *D. invisus*–IgG2 responses had greater risk for progression to T1D diagnosis and were more likely to benefit from

Table 2. Baseline ACAb responses improve performance of Cox models in predicting T1D diagnosis. The addition of baseline ACAb responses improved model performance, as evaluated by integrated time-dependent AUCs, Akaike information criterion (AIC), and the partial likelihood test against reduced models limited to treatment arm, age, BMI, *HLA-DR4*, or C-peptide value as predictor variables.

	Predictors	Integrated AUC	AIC	*P* value
Model 1	Treatment.Arm	0.59	238.51	–
Model 2	Age + Treatment.Arm	0.63	237.42	(vs. model 1) 0.0318
Model 3	Treatment.Arm*DR4 + Age	0.70	232.61	(vs. model 2) 0.01
Model 4	Treatment.Arm*DR4 + Age + Di.IgG2*DR4	0.73	231.15	(vs. model 3) 0.04
Model 5	Treatment.Arm + Age + BMI + mu_cpep	0.68	234.61	(vs. model 2) 0.009
Model 6	Treatment.Arm + Age + BMI + mu_cpep + Ef.IgG2	0.72	230.84	(vs. model 5) 0.009
Model 7	Treatment.Arm + Age + BMI + mu_cpep + Bl.IgG2	0.71	231.23	(vs. model 5) 0.02

teplizumab treatment, whereas the converse trend was observed in *HLA-DR4*$^-$ individuals.

ACAb responses associated with T1D progression contribute to disease risk prediction

The longitudinal design of the TN-10 trial allowed us to use time-dependent models to explore associations between ACAb responses and time to T1D diagnosis (*43*). Because ACAb responses were stable over time in both treatment arms (fig. S3), inclusion of later time points increased power to detect ACAb response associations with time to T1D diagnosis. Such time-dependent Cox models also provide a complementary approach to landmark analysis for addressing immortal time bias (*34*, *46*). As we had observed in single–time point analysis, controlling for age, sex, BMI, treatment arm, and *HLA-DR*, higher *B. longum*– and *E. faecalis*–IgG2 responses evident at any time before or after treatment arm randomization were associated with increased risk of T1D diagnosis (Fig. 7A, $P = 0.006$ and Fig. 7B, $P = 0.015$, respectively). Given the association of time-dependent ACAb responses with risk of T1D diagnosis, we compared these two ACAb responses with C-peptide values for their performance in predicting time to T1D diagnosis. An increase in C-peptide before or after the randomization, controlling for prespecified variables, was associated with decreased risk of T1D diagnosis (Fig. 7C), consistent with prior evidence that higher C-peptide values reflect preservation of β cell function.

In contrast to *B. longum*– and *E. faecalis*–IgG2 responses, whose associations with time to T1D diagnosis were significant in the entire TN-10 cohort, *D. invisus*–IgG2 responses were differentially associated with risk of progressing to T1D diagnosis in *HLA-DR4*$^+$ versus *HLA-DR4*$^-$ participants (Fig. 7D). In *HLA-DR4*$^-$ participants, an increase in *D. invisus*–IgG2 was associated with a decreased risk of T1D diagnosis (*D. invisus*–IgG2 $P = 0.02$). For *HLA-DR4*$^+$ but not *HLA-DR4*$^-$ individuals, *D. invisus*–IgG2 responses were positively associated with a future T1D diagnosis (*D. invisus*–IgG2–*HLA-DR4* interaction $P = 0.005$). These results reveal the influence of *HLA-DR4* on the association between *D. invisus*–IgG2 responses and time to T1D diagnosis, in agreement with our observations in the single–time point analysis.

The previous analysis approach estimated the average hazards over time associated with repeated ACAb measures. To evaluate the association between longitudinal ACAb and time to T1D diagnosis, joint models were used for longitudinal and time-to-event data (*47*, *48*). For each ACAb response, we normalized measurements of all participants from all time points into a standard normal distribution and used linear mixed models to estimate time effects (*49*). Survival data were modeled to account for treatment arms, age, sex, BMI, and *HLA-DR* genotype. Longitudinal *B. longum*–IgG2 (HR = 1.99, $P = 0.002$) and *E. faecalis*–IgG2 (HR = 1.76, $P = 0.008$) responses, as well as the interaction between *D. invisus*–IgG2 responses and *HLA-DR4* (HR = 2.79, $P = 0.015$), were associated with risk of T1D diagnosis.

We used the joint models to calculate the expected probability of remaining T1D-free for selected individuals combining baseline characteristics and longitudinal *B. longum*–IgG2 (fig. S5A), *E. faecalis*–IgG2 (fig. S5B), or *D. invisus*–IgG2 (fig. S5, C and D) responses. These trends were consistent with single–time point analyses. Longitudinal analyses suggested that ACAb responses were stable over time and consistently associated with risk of future T1D diagnoses. We then asked whether ACAb responses at baseline, in addition to *HLA-DR4* haplotype and baseline C-peptide values, provided predictive value for a future T1D diagnosis. We used incident/dynamic time-dependent area under the receiver operating characteristic (ROC) curve (AUC), Akaike information criterion (AIC), and partial likelihood ratio test to compare performance of models incorporating baseline characteristics, treatment arm, and ACAb responses in predicting T1D diagnosis (Table 2) (*50*–*54*). These models demonstrate that an interaction between *HLA-DR4* genotype and *D. invisus*–IgG2 responses improved prediction of T1D diagnosis compared with *HLA-DR4* genotype alone (Fig. 8, A and B). Moreover, *B. longum*– and *E. faecalis*–IgG2 responses independently improved T1D diagnosis prediction compared with only C-peptide value (Fig. 8, C and D). The improved AUC by incorporation of ACAb responses suggested that their inclusion as markers may aid participant selection in future T1D prevention trials.

Validation in an independent cohort

Last, we sought to validate associations observed in TN-10 between ACAb responses and time to diabetes diagnosis in an independent study cohort. Because TN-10 is the only trial in which teplizumab has been tested for T1D prevention, we prioritized independent assessment of associations between the specific ACAb responses, *HLA-DR4* (a predictor of teplizumab response in TN-10), and time to T1D diagnosis. Pathways to Prevention (TN-01) is an observational study of nondiabetic relatives of persons with T1D who receive frequent screening for IAB (*55*). We accessed serum samples from prediabetic TN-01 participants ($n = 61$) with two IABs who later progressed to diabetes diagnosis. The time to diagnosis/last follow-up in this validation cohort [median (interquartile range, IQR): 343.76 (176.87) days] was significantly shorter than

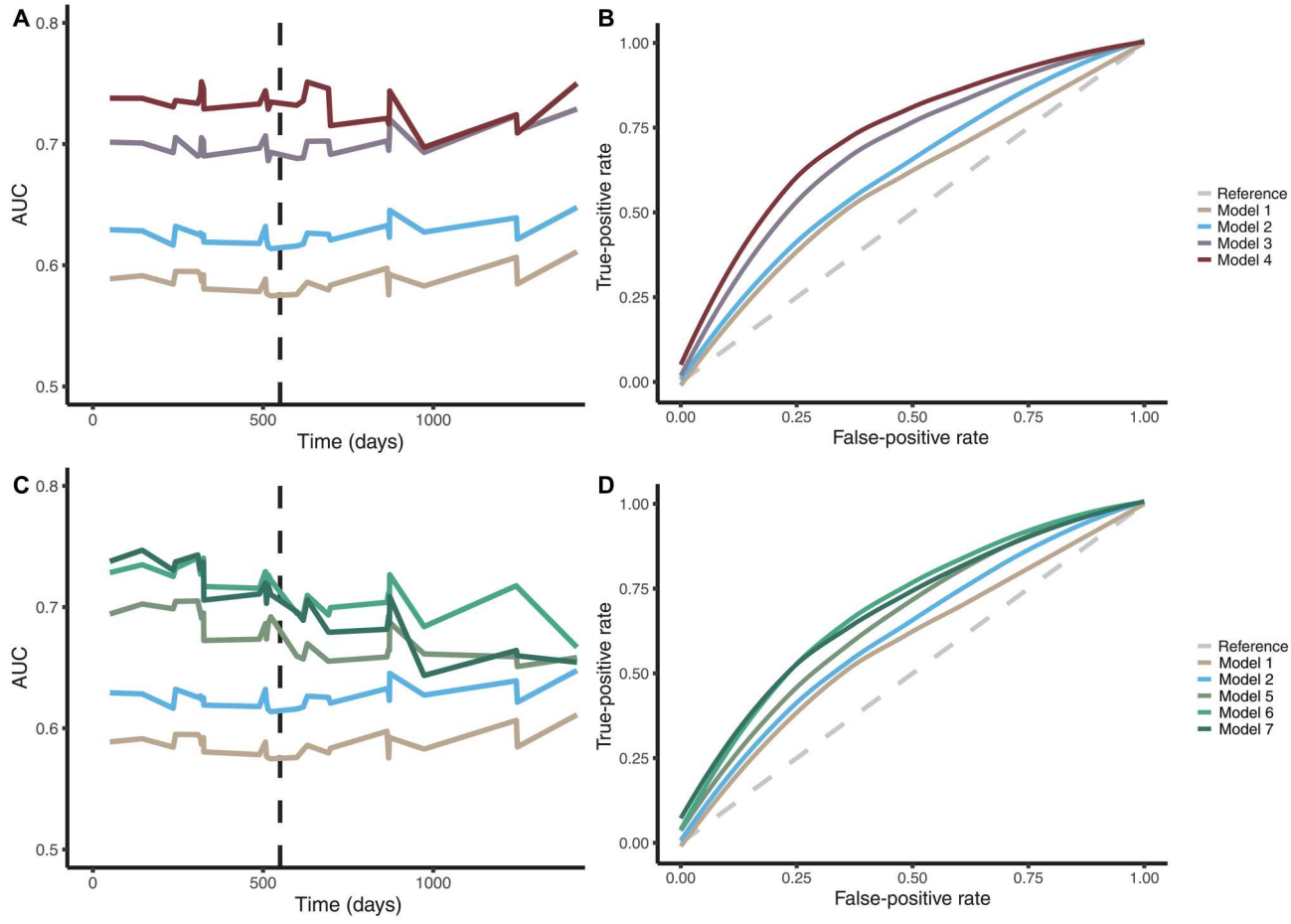

Fig. 8. Baseline ACAb responses improve performance of Cox models in predicting T1D diagnosis. Time-dependent AUCs (**A**) and ROC curves (**B**) of models using one or more of treatment arm, age, *HLA-DR4*, and baseline *D. invisus*–IgG2 responses as covariates for T1D diagnosis prediction after randomization. Time-dependent AUCs (**C**) and ROC curves (**D**) of models using one or more of treatment arm, age, BMI, C-peptide value, baseline *B. longum*–IgG2 responses, and baseline *E. faecalis*–IgG2 responses as covariates for T1D diagnosis prediction. Vertical dotted lines mark 550 days, the collection time of the last follow-up sample for which ROC curves were generated. The specification of variables included in each model is listed in Table 2. The covariates were incorporated into these models using a step-up procedure and included only if they improved the partial log likelihood of the model at α = 0.1 level (two-sided).

that in TN-10 trial participants [median (IQR): 1101 (1123) days; $P = 1.8 \times 10^{-14}$, Wilcoxon rank sum test; fig. S6]. Despite this difference and sample size, we observed an interaction between ACAb responses and carriage of *HLA-DR4*. In the validation cohort, the risk of progression to T1D diagnosis in *HLA-DR4*$^+$ versus *HLA-DR4* participants differed on the basis of magnitude of *B. longum*–IgG2 responses (fig. S7, $P = 0.03$). The low *B. longum*–IgG2 response subgroup (fig. S7A) showed no significant difference between *HLA-DR4*$^+$ versus *HLA-DR4* participants in time to T1D diagnosis. In contrast, in the high *B. longum*–IgG2 response subgroup, *HLA-DR4*$^+$ participants displayed significantly longer time to T1D diagnosis ($P = 0.03$) (fig. S7B). We observed a similar association for IgA responses to *D. invisus*, which correlated with IgG2 responses to *D. invisus* in both cohorts (fig. S8C, TN-01: $P = 0.0006$; TN-10: $P = 2.6 \times 10^{-7}$).

The differential distribution of time to T1D diagnosis in *HLA-DR4*$^+$ participants was evident in the high *D. invisus*–IgA response subgroup (fig. S8B; $P = 0.04$). The lack of significant association between *D. invisus*–IgG2 response and *HLA-DR4* that we had observed in the TN-10 samples may reflect the narrow range of time to T1D diagnosis in the TN-01 validation cohort. In the TN-10 trial, *HLA-DR4* was associated with response to teplizumab, which in turn delayed time to diabetes diagnosis. The far more restricted time interval to diagnosis in TN-01 validation compared with TN-10 participants limited direct comparisons of the *HLA-DR4* effect between the two cohorts. With this caveat, these TN-01 validation data concur with our previously reported *HLA-DR*–dependence of ACAb responses associated with T1D risk (*28*). The TN-01 cohort results substantiate the observed associations of *B. longum* and *D. invisus* ACAb responses with time to diabetes diagnosis and support the value of these responses for prediction of teplizumab response in the TN-10 participants.

DISCUSSION

Teplizumab delayed T1D diagnosis in the TN-10 trial of relatives of patients who displayed IABs and dysglycemia at baseline (*10*, *25*, *26*). On the basis of these outcomes, the FDA recently approved teplizumab for treatment of at-risk prediabetic patients (*27*). However, like many immunotherapies (*2*, *3*, *7*, *9*, *11*, *56*), participant

responses to teplizumab were heterogeneous. Participant age, *HLA-DR* genotype, and IAB specificities were associated with treatment response (*10*). In a prior trial in new-onset diabetics, the activity of teplizumab was associated with greater frequencies of $CD8^+$ T cells that coexpress inhibitory receptors suggestive of partial "exhaustion" (*21*). In a humanized mouse model reconstituted with human hematopoietic cells, teplizumab treatment promoted xenograft tolerance, accompanied by production of immunoregulatory IL-10 in gut lymphoid tissues. Induction of graft tolerance was compromised when these mice were preconditioned with an antibiotic cocktail that altered gut microbiome composition (*57*). Moreover, in this model, teplizumab treatment elicited human gut-tropic T cell migration to the intestine and production of IL-10 (*24*). Collectively, findings in human trials and in humanized mouse models implicate a relationship between teplizumab's activity and gut-associated immune responses where bacterial antigens are abundant. Thus, we examined ACAb in the TN-10 cohort from randomization and up to 18 months before T1D diagnosis to evaluate their associations with disease progression and teplizumab effect.

We identified three ACAb responses before and after randomization that were associated with progression to T1D in the TN-10 cohort. First, higher IgG2 responses to *B. longum* and *E. faecalis* were associated with higher risk of progression to T1D when all participants were considered together. A higher ACAb response observed before T1D diagnosis may reflect enhanced intestinal permeability enabling immune exposure to bacterial antigens, consistent with reports in cohorts of prediabetic and recently diagnosed individuals (*58*–*60*). Second, we observed that higher IgG2 antibody responses to *B. longum* were associated with time to T1D diagnosis in the TN-10 cohort. These data support previous suggestions that T1D is associated with gut microbial responses that produce a noninflammatory, homeostatic state (*45*, *61*–*63*). A prominent member of early-life microbiota, *B. longum* can metabolize human milk oligosaccharides and persists in adult gut microbiota (*64*–*67*). A previous longitudinal study of fecal microbiome composition in infants and young children at risk for T1D suggested that insufficient early immune exposure to this species is associated with increased T1D risk (*67*). In contrast to *B. longum*, *E. faecalis* can serve both as a probiotic that regulates infant inflammatory immune responses (*68*, *69*) and as a pathogen that exacerbates inflammatory responses and impairs barrier integrity in settings of inflammatory bowel and graft-versus-host diseases (*70*–*72*). These variable impacts of *E. faecalis* underscore the dependence of immune responses to the gut bacteria on both microbial community composition and the tone of immune responses in the intestinal mucosa. The dynamic relationships within the intestinal microbial community and between which and the mucosal immune system may be uniquely affected by immunomodulatory treatment, such as teplizumab, whose effect on the microbial community is difficult to predict ex vivo and requires clinical investigations to understand. The third association we found was an *HLA-DR4*–dependent association between *D. invisus*–IgG2 responses and progression to T1D diagnosis. The *HLA-DR4* effect on the magnitude of the *D. invisus*–reactive antibodies in the TN-10 participants suggests a role for T cell help in their formation. *D. invisus* abundance in the gut has been reported to be associated with risk for both T1D and celiac disease (*44*, *45*, *73*). On the basis of our observations of *D. invisus*–IgG2 responses, the association of this organism with both diseases likely reflects their shared contribution of *HLA-DR4*. Both the *B. longum*– and *HLA-DR4*–dependent associations with time to T1D diagnosis were validated in the independent TN-01 study cohort.

We found that the same ACAb responses that were associated with progression to T1D could also predict treatment responses to teplizumab before randomization. The difference in treatment effect between subgroups stratified by baseline ACAb suggests that immune responses to the gut microbiota are connected to the mechanism of action of teplizumab in the context of T1D prevention. Teplizumab displayed a more beneficial effect on participants who were further progressed toward T1D onset, because treatment effect was more evident in participant subgroups defined by high baseline *B. longum*– or *E. faecalis*–IgG2 responses. Moreover, we report an interaction between *HLA-DR4*, an established disease risk marker and predictor of treatment response, and *D. invisus*–IgG2 responses, which provided additional features to stratify at-risk individuals for treatment. The clinical relationship between ACAb responses and progression to islet autoimmunity or T1D are unknown, and as single measures displayed a modest clinical impact (as assessed by HRs) in the TN-10 analysis. However, the robust association of ACAb responses, independently (*B. longum* and *E. faecalis*) or in interaction with *HLA-DR* (*D. invisus*) to treatment response and time to T1D, may reflect T cell involvement in mediating response to the gut microbiota and reactivity to the islet tissue. Titers of both anti-IAB and ACAb antibodies remained stable over time and were not altered by the single course of teplizumab. Thus, these antibody responses can provide reliable markers that add predictive value to defined risk markers *HLA-DR4* and C-peptide for early identification of individuals at risk and who may benefit from this treatment.

There are several limitations to the current study. TN-10 ($n = 76$) was designed to detect teplizumab treatment effect and was not powered to discover associations between treatment effect and biomarkers (*74*) that could reveal mechanisms underlying heterogeneous treatment responses. The participants available for this study ($n = 63$) were representative of the full trial cohort; however, the sample size may have limited our capacity to identify additional ACAb responses that may also be associated with time to T1D diagnosis. In addition, because the TN-10 participants were >95% non-Hispanic Caucasian (*10*), these data do not address ACAb responses associated with T1D progression in other ethnic groups. T1D has been most extensively studied in individuals of European ancestry, but studies show greater recent increases in disease incidences, difference in genetic architecture, and poorer glycemic control in African Americans and Hispanic individuals (*75*–*80*). A gap in knowledge will remain until ACAb analyses are performed in demographically diverse groups to assess population-based variations in the specificity or magnitude of immune responses against gut microbes. Last, our validation cohort allowed us to address the generalizability of the ACAb responses in predicting time to T1D diagnosis in individuals who are contemporaneous to participants in the TN-10 trial and confirmed our previous observations (*28*). We could not assess the effects of teplizumab in this second cohort because there has only been a single study of this intervention in prevention. Next steps include operationalizing a defined ACAb assay platform across clinical trial and research sites to guide participant recruitment and adaptation into clinical laboratory settings.

In summary, we show that immune responses to common intestinal microbes are associated with progression to T1D diagnosis in

the context of an immunotherapy that delayed disease onset. ACAb responses identified at recruitment of the TN-10 trial were predictive of teplizumab responders. Thus, ACAb responses have the potential to guide the recruitment of individuals for T1D trials and offer approaches to identify markers to untangle the heterogeneity in response to immunotherapies. At a mechanistic level, the ACAb responses defined here provide past records of exposure to the gut microbial community and support independent evidence that T1D risk is affected by early-life factors that modify the gut microbiota and, especially, their interaction with the host immune system.

MATERIALS AND METHODS

Study design

We studied nondiabetic relatives of patients with T1D (n = 63) between 8 and 49 years of age that comprised a subgroup of the entire cohort (n = 76) enrolled in the TN-10 trial (NCT01030861). This subgroup was selected on the basis of the availability of serial serum samples for analysis. The TN-10 trial was a phase 2, randomized, placebo-controlled, double-blind trial to test the efficacy of a single course of teplizumab treatment on time to T1D in at-risk individuals with evidence of early dysglycemia and at least two types of IAB. The details and clinical outcomes of the TN-10 trial have been reported (*10*). The use of samples for this study was approved by the Research Ethics Boards at the Hospital for Sick Children (REB no. 1000057146). The data presented here consist of ACAb responses generated from samples collected at baseline and at 6, 12, and 18 months after randomization, C-peptide values obtained from oral glucose tolerance test at matching time points, and participant characteristics at baseline. C-peptide AUC was calculated using the trapezoidal rule and divided by 120, the duration of the oral glucose tolerance test in minutes.

IAB assays

All IAB essays to define GADA, IA2A, mIAA, and ZnT8A positivity used well-established methods *(81*, *82)* and were performed at the Barbara Davis Diabetes Center (Denver, CO). IAB positivity was defined using threshold indexes of GADA > 20, IA2A > 5, mIAA > 0.01, and ZnT8A > 0.02.

ACAb assays

The ACAb assay platform was used to define the response index for each serum sample, bacterial target, and antibody isotype combination. Stool sample collection was not included in TN-10. The ACAb platform was replicated once on the TN-10 samples. The technical replicates reproduced the results shown here. We used a collection of well-characterized human bacterial strains isolated from fecal samples representative of the gut microbiota in healthy humans (table S1 and Fig. 2). The *Escherichia coli* strain was from the American Type Culture Collection. This bacterial collection included representatives of the four most abundant bacteria phyla in the human gut microbiota, Firmicutes, Actinobacteria, Bacteroidetes, and Proteobacteria. With the exception of *E. coli*, multiple strains of each species were used to capture potential strain-specific antigen complexity. For each species, the strains were grown individually and pooled in equal abundance before labeling for the ACAb assay. Details of the ACAb assay have been previously reported (*28*). Briefly, each serum sample was serially diluted four times, incubated with two freshly cultured bacteria species at equal concentration based on optical density measurements, and stained with one of the amine-reactive dyes CellTrace carboxyfluorescein diacetate succinimidyl ester (CFSE) or Violet (Thermo Fisher Scientific), respectively. After washing, fluorochrome-labeled anti-IgG1 (SouthernBiotech, catalog no. 9052-09, RRID: AB_2796621), IgG2 (SouthernBiotech, catalog no. 9070-31, RRID: AB_2796641), and IgA (Jackson ImmunoResearch Laboratories, catalog no. 109-585-011, RRID: AB_2337859) secondary antibodies were added to the serum-incubated bacteria to qualify the percentage of bacteria bound by serum antibodies using flow cytometry. For each ACAb assay, serum samples from the 63 TN-10 participants were incubated with a specific pair of labeled bacteria species and fixed by addition of paraformaldehyde to a final concentration of 2% on the same day, and the data were acquired by flow cytometry within 2 days. The staining efficiencies of CellTrace CFSE and Violet were tested for each bacterial culture and were required to be >75% for all strains on the day of the experiment to ensure bacteria viability. Samples were acquired on LSRFortessa (BD Biosciences) with FACSDiva software. The instrument was standardized daily by adjusting the voltages for photomultiplier tube using rainbow beads (Spherotech). The flow cytometry standard files were analyzed in FlowJo (v10.8.1).

Response index calculation

The percentage of anti-isotype antibody–coated bacteria (Ab+%) was calculated for each serum dilution, bacterial target, and isotype. Ab+% was then plotted on the y axis against log-transformed serum dilutions on the x axis. A spline model was used to generate a dilution curve of the ACAb response for each bacterial target and isotype, and the AUC was used as the response index.

Serum antibody quantification

The total IgG1, IgG2, and IgA antibodies in TN-10 samples were quantified using the enzyme-linked immunosorbent assay (ELISA; IgG1 and IgA: MyBioSource; IgG2: Thermo Fisher Scientific). The mean and SD of IgG1, IgG2, and IgA serum concentrations were 15.808 ± 6.74, 1.46 ± 1.12, and 4.11 ± 3.82 mg/ml, respectively.

Statistical analyses

All analyses for this study were completed in R (v3.6.2) (*83*). Duplicated samples (n = 2) were removed from analysis. The difference in baseline characteristics (Table 1) was tested by Fisher's exact test for categorical variables and Welch two-sample t test assuming unequal variance for continuous variables using stats. The baseline ACAbs, unscaled or scaled by caret (v6.0-85), were selected by Cox models with boosting (mboost v2.9-5; CoxBoost v1.4), with baseline characteristics (age, sex, BMI, *HLA-DR*, treatment arm, and C-peptide AUC) as mandatory variables (*36*). The time to event distribution for each stratum (for example, high versus low *B. longum*–IgG2 response) was estimated by Kaplan-Meier analysis (*30*). The effects of baseline, 6-month, and longitudinal covariates on time to T1D, as well as the treatment effects in subgroups, were estimated by multivariate linear Cox proportional-hazards (PH) regression adjusting for age, sex, BMI, treatment arms, and *HLA-DR* (*34*). The adjusted P value cutoff based on effective number of independent tests for estimating effect of interaction between 6-month ACAbs and *HLA-DR* on time to T1D was calculated by matrix spectral decomposition (*84*). All single–time point survival analyses had modified time to

event based on landmark time, and model assumptions were validated using survival (v3.3-1) (*85*–*87*). Where the assumptions of PH did not hold, an additive Cox model with smoothing function was used to estimate the effect of the covariate. The linear mixed models were fitted with nlme (v3.1-155) (*49*). The joint models for longitudinal and time-to-event data were fitted using JM (v1.5-2) (*48*). The incident/dynamic time-dependent AUC for Cox models was evaluated using risksetROC (v1.0.4) (*51*). The partial likelihood ratio test and AIC for comparison between Cox models are completed using nonnestcox (v0.0.0.9) with a nested option (*54*). $P < 0.05$ was considered significant unless stated otherwise.

Supplementary Materials

This PDF file includes:
Figs. S1 to S8
Table S1

Other Supplementary Material for this manuscript includes the following:
Data file S1
MDAR Reproducibility Checklist

REFERENCES AND NOTES

1. S. L. Hauser, E. Waubant, D. L. Arnold, T. Vollmer, J. Antel, R. J. Fox, A. Bar-Or, M. Panzara, N. Sarkar, S. Agarwal, A. Langer-Gould, C. H. Smith; HERMES Trial Group, B-cell depletion with rituximab in relapsing–remitting multiple sclerosis. *N. Engl. J. Med.* **358**, 676–688 (2008).
2. K. Hawker, P. O'Connor, M. S. Freedman, P. A. Calabresi, J. Antel, J. Simon, S. Hauser, E. Waubant, T. Vollmer, H. Panitch, J. Zhang, P. Chin, C. H. Smith; OLYMPUS trial group, Rituximab in patients with primary progressive multiple sclerosis: Results of a randomized double-blind placebo-controlled multicenter trial. *Ann. Neurol.* **66**, 460–471 (2009).
3. C. G. Chisari, E. Sgarlata, S. Arena, S. Toscano, M. Luca, F. Patti, Rituximab for the treatment of multiple sclerosis: A review. *J. Neurol.* **269**, 159–183 (2022).
4. C. N. Ellis, G. G. Krueger; Alefacept Clinical Study Group, Treatment of chronic plaque psoriasis by selective targeting of memory effector T lymphocytes. *N. Engl. J. Med.* **345**, 248–255 (2001).
5. G. G. Krueger, K. P. Callis, Development and use of alefacept to treat psoriasis. *J. Am. Acad. Dermatol.* **49**, 87–97 (2003).
6. P. E. Lipsky, D. M. F. M. van der Heijde, E. W. St Clair, D. E. Furst, F. C. Breedveld, J. R. Kalden, J. S. Smolen, M. Weisman, P. Emery, M. Feldmann, G. R. Harriman, R. N. Maini; Anti-Tumor Necrosis Factor Trial in Rheumatoid Arthritis with Concomitant Therapy Study Group, Infliximab and methotrexate in the treatment of rheumatoid arthritis. Anti-tumor necrosis factor trial in rheumatoid arthritis with concomitant therapy study group. *N. Engl. J. Med.* **343**, 1594–1602 (2000).
7. P. Conigliaro, P. Triggianese, E. De Martino, G. L. Fonti, M. S. Chimenti, F. Sunzini, A. Viola, C. Canofari, R. Perricone, Challenges in the treatment of rheumatoid arthritis. *Autoimmun. Rev.* **18**, 706–713 (2019).
8. S. B. Hanauer, B. G. Feagan, G. R. Lichtenstein, L. F. Mayer, S. Schreiber, J. F. Colombel, D. Rachmilewitz, D. C. Wolf, A. Olson, W. Bao, P. Rutgeerts; ACCENT I Study Group, Maintenance infliximab for crohn's disease: The accent I randomised trial. *Lancet* **359**, 1541–1549 (2002).
9. S. Ben-Horin, U. Kopylov, Y. Chowers, Optimizing anti-TNF treatments in inflammatory bowel disease. *Autoimmun. Rev.* **13**, 24–30 (2014).
10. K. C. Herold, B. N. Bundy, S. A. Long, J. A. Bluestone, L. A. DiMeglio, M. J. Dufort, S. E. Gitelman, P. A. Gottlieb, J. P. Krischer, P. S. Linsley, J. B. Marks, W. Moore, A. Moran, H. Rodriguez, W. E. Russell, D. Schatz, J. S. Skyler, E. Tsalikian, D. K. Wherrett, A.-G. Ziegler, C. J. Greenbaum; Type 1 Diabetes TrialNet Study Group, An anti-CD3 antibody, teplizumab, in relatives at risk for type 1 diabetes. *N. Engl. J. Med.* **381**, 603–613 (2019).
11. M. Battaglia, S. Ahmed, M. S. Anderson, M. A. Atkinson, D. Becker, P. J. Bingley, E. Bosi, T. M. Brusko, L. A. DiMeglio, C. Evans-Molina, S. E. Gitelman, C. J. Greenbaum, P. A. Gottlieb, K. C. Herold, M. J. Hessner, M. Knip, L. Jacobsen, J. P. Krischer, S. A. Long, M. Lundgren, E. F. McKinney, N. G. Morgan, R. A. Oram, T. Pastinen, M. C. Peters, A. Petrelli, X. Qian, M. J. Redondo, B. O. Roep, D. Schatz, D. Skibinski, M. Peakman, Introducing the endotype concept to address the challenge of disease heterogeneity in type 1 diabetes. *Diabetes Care* **43**, 5–12 (2020).
12. G. S. Eisenbarth, Banting Lecture 2009: An unfinished journey: Molecular pathogenesis to prevention of type 1A diabetes. *Diabetes* **59**, 759–774 (2010).
13. M. A. Atkinson, G. S. Eisenbarth, A. W. Michels, Type 1 diabetes. *Lancet* **383**, 69–82 (2014).
14. A. Pugliese, Autoreactive T cells in type 1 diabetes. *J. Clin. Invest.* **127**, 2881–2891 (2017).
15. L. A. Ferrat, K. Vehik, S. A. Sharp, Å. Lernmark, M. J. Rewers, J.-X. She, A.-G. Ziegler, J. Toppari, B. Akolkar, J. P. Krischer, M. N. Weedon, R. A. Oram, W. A. Hagopian; TEDDY Study Group, A combined risk score enhances prediction of type 1 diabetes among susceptible children. *Nat. Med.* **26**, 1247–1255 (2020).
16. C. M. Dayan, R. E. Besser, R. A. Oram, W. Hagopian, M. Vatish, O. Bendor-Samuel, M. D. Snape, J. A. Todd, Preventing type 1 diabetes in childhood. *Science* **373**, 506–510 (2021).
17. J. P. Krischer, X. Liu, Å. Lernmark, W. A. Hagopian, M. J. Rewers, J.-X. She, J. Toppari, A.-G. Ziegler, B. Akolkar; TEDDY Study Group, Predictors of the initiation of islet autoimmunity and progression to multiple autoantibodies and clinical diabetes: The teddy study. *Diabetes Care* **45**, 2271–2281 (2022).
18. C. K. Boughton, J. M. Allen, J. Ware, M. E. Wilinska, S. Hartnell, A. Thankamony, T. Randell, A. Ghatak, R. E. J. Besser, D. Elleri, N. Trevelyan, F. M. Campbell, J. Sibayan, P. Calhoun, R. Bailey, G. Dunseath, R. Hovorka; CLOuD Consortium, Closed-loop therapy and preservation of C-peptide secretion in type 1 diabetes. *N. Engl. J. Med.* **387**, 882–893 (2022).
19. K. C. Herold, W. Hagopian, J. A. Auger, E. Poumian-Ruiz, L. Taylor, D. Donaldson, S. E. Gitelman, D. M. Harlan, D. Xu, R. A. Zivin, J. A. Bluestone, Anti-CD3 monoclonal antibody in new-onset type 1 diabetes mellitus. *N. Engl. J. Med.* **346**, 1692–1698 (2002).
20. J. E. Tooley, N. Vudattu, J. Choi, C. Cotsapas, L. Devine, K. Raddassi, M. R. Ehlers, J. G. McNamara, K. M. Harris, S. Kanaparthi, D. Phippard, K. C. Herold, Changes in T-cell subsets identify responders to FCR-nonbinding anti-CD3 MAB (teplizumab) in patients with type 1 diabetes. *Eur. J. Immunol.* **46**, 230–241 (2015).
21. S. A. Long, J. Thorpe, H. A. DeBerg, V. Gersuk, J. A. Eddy, K. M. Harris, M. Ehlers, K. C. Herold, G. T. Nepom, P. S. Linsley, Partial exhaustion of CD8 T cells and clinical response to teplizumab in new-onset type 1 diabetes. *Sci. Immunol.* **1**, eaai7793 (2016).
22. S. A. Long, J. Thorpe, K. C. Herold, M. Ehlers, S. Sanda, N. Lim, P. S. Linsley, G. T. Nepom, K. M. Harris, Remodeling T cell compartments during anti-CD3 immunotherapy of type 1 diabetes. *Cell. Immunol.* **319**, 3–9 (2017).
23. A. L. Perdigoto, P. Preston-Hurlburt, P. Clark, S. A. Long, P. S. Linsley, K. M. Harris, S. E. Gitelman, C. J. Greenbaum, P. A. Gottlieb, W. Hagopian, A. Woodwyk, J. Dziura, K. C. Herold; Immune Tolerance Network, The immune tolerance network, treatment of type 1 diabetes with teplizumab: Clinical and immunological follow-up after 7 years from diagnosis. *Diabetologia* **62**, 655–664 (2019).
24. F. Waldron-Lynch, O. Henegariu, S. Deng, P. Preston-Hurlburt, J. Tooley, R. Flavell, K. C. Herold, Teplizumab induces human gut-tropic regulatory cells in humanized mice and patients. *Sci. Transl. Med.* **4**, 118ra12 (2012).
25. E. K. Sims, B. N. Bundy, K. Stier, E. Serti, N. Lim, S. A. Long, S. M. Geyer, A. Moran, C. J. Greenbaum, C. Evans-Molina, K. C. Herold, Teplizumab improves and stabilizes beta cell function in antibody-positive high-risk individuals. *Sci. Transl. Med.* **13**, eabc8980 (2021).
26. E. K. Sims, D. Cuthbertson, K. C. Herold, J. M. Sosenko, The deterrence of rapid metabolic decline within 3 months after teplizumab treatment in individuals at high risk for type 1 diabetes. *Diabetes* **70**, 2922–2931 (2021).
27. Office of the Commissioner, FDA approves first drug that can delay onset of type 1 diabetes. U.S. Food and Drug Administration (2022); www.fda.gov/news-events/press-announcements/fda-approves-first-drug-can-delay-onset-type-1-diabetes.
28. A. Paun, C. Yau, S. Meshkibaf, M. C. Daigneault, L. Marandi, S. Mortin-Toth, A. Bar-Or, E. Allen-Vercoe, P. Poussier, J. S. Danska, Association of HLA-dependent islet autoimmunity with systemic antibody responses to intestinal commensal bacteria in children. *Sci. Immunol.* **4**, eaau8125 (2019).
29. H. Siljander, J. Honkanen, M. Knip, Microbiome and type 1 diabetes. *EBioMedicine* **46**, 512–521 (2019).
30. E. L. Kaplan, P. Meier, Nonparametric estimation from incomplete observations. *J. Am. Stat. Assoc.* **53**, 457–481 (1958).
31. K. Murphy, C. Weaver, A. Mowat, L. Berg, D. Chaplin, *D. Janeway's Immunobiology* (Garland Science, Taylor & Francis Group, 2017).
32. J. R. Anderson, K. C. Cain, R. D. Gelber, Analysis of survival by tumor response. *J. Clin. Oncol.* **1**, 710–719 (1983).
33. M. . Buyse, P. Piedbois, On the relationship between response to treatment and survival time. *Stat. Med.* **15**, 2797–2812 (1996).
34. S. Suissa, Immortal time bias in pharmacoepidemiology. *Am. J. Epidemiol.* **167**, 492–499 (2008).
35. C. J. Morgan, Landmark analysis: A primer. *J. Nucl. Cardiol.* **26**, 391–393 (2019).

36. R. De Bin, Boosting in Cox regression: A comparison between the likelihood-based and the model-based approaches with focus on the R-packages CoxBoost and mboost. *Comput Stat* **31**, 513–531 (2016).
37. D. R. Cox, Regression models and life-tables. *J. R. Stat. Soc. B. Methodol.* **34**, 187–202 (1972).
38. D. F. Steiner, D. Cunningham, L. Spigelman, B. Aten, Insulin biosynthesis: Evidence for a precursor. *Science* **157**, 697–700 (1967).
39. J. P. Palmer, G. A. Fleming, C. J. Greenbaum, K. C. Herold, L. D. Jansa, H. Kolb, J. M. Lachin, K. S. Polonsky, P. Pozzilli, J. S. Skyler, M. W. Steffes, C-peptide is the appropriate outcome measure for type 1 diabetes clinical trials to preserve β-cell function. *Diabetes* **53**, 250–264 (2004).
40. A. P. Lambert, K. M. Gillespie, G. Thomson, H. J. Cordell, J. A. Todd, E. A. M. Gale, P. J. Bingley, Absolute risk of childhood-onset type 1 diabetes defined by human leukocyte antigen class ii genotype: A population-based study in the United Kingdom. *J. Clin. Endocrinol. Metabol.* **89**, 4037–4043 (2004).
41. H. Erlich, A. M. Valdes, J. Noble, J. A. Carlson, M. Varney, P. Concannon, J. C. Mychaleckyj, J. A. Todd, P. Bonella, A. L. Fear, E. Lavant, A. Louey, P. Moonsamy; CLOuD ConsortiuType 1 Diabetes Genetics Consortium, HLA DR-DQ haplotypes and genotypes and type 1 diabetes risk: Analysis of the type 1 diabetes genetics consortium families. *Diabetes* **57**, 1084–1092 (2008).
42. J. A. Noble, A. M. Valdes, Genetics of the HLA region in the prediction of type 1 diabetes. *Curr. Diab. Rep.* **11**, 533–542 (2011).
43. M. P. Morran, A. Vonberg, A. Khadra, M. Pietropaolo, Immunogenetics of type 1 diabetes mellitus. *Mol. Aspects Med.* **42**, 42–60 (2015).
44. E. Bosi, L. Molteni, M. G. Radaelli, L. Folini, I. Fermo, E. Bazzigaluppi, L. Piemonti, M. R. Pastore, R. Paroni, Increased intestinal permeability precedes clinical onset of type 1 diabetes. *Diabetologia* **49**, 2824–2827 (2006).
45. A. D. Kostic, D. Gevers, H. Siljander, T. Vatanen, T. Hyötyläinen, A.-M. Hämäläinen, A. Peet, V. Tillmann, P. Pöhö, I. Mattila, H. Lähdesmäki, E. A. Franzosa, O. Vaarala, M. de Goffau, H. Harmsen, J. Ilonen, S. M. Virtanen, C. B. Clish, M. Oreši, C. Huttenhower, M. Knip; DIABIMMUNE Study Group, R. J. Xavier, The dynamics of the human infant gut microbiome in development and in progression toward type 1 diabetes. *Cell Host Microbe* **17**, 260–273 (2015).
46. T. Therneau, C. Crowson, E. Atkinson, Using time dependent covariates and time dependent coefficients in the Cox model (2022); https://cran.rstudio.com/web/packages/survival/vignettes/timedep.pdf.
47. D. Rizopoulos, *Joint Models for Longitudinal and Time-to-Event Data: With Applications in R* (Chapman & Hall/CRC, 2012).
48. D. Rizopoulos, JM: An R Package for the joint modelling of longitudinal and time-to-event data. *J. Stat. Softw.* **35**, 1–33 (2010).
49. J. Pinheiro, D. Bates, S. DebRoy, D. Sarkar, R Core Team. nlme: Linear and nonlinear mixed effects models (2022); https://CRAN.R-project.org/package=nlme.
50. P. J. Heagerty, Y. Zheng, Survival model predictive accuracy and ROC curves. *Biometrics* **61**, 92–105 (2005).
51. P. J. Heagerty, P. Saha-Chaudhuri. risksetROC: Riskset ROC curve estimation from censored survival data (2022); https://CRAN.R-project.org/package=risksetROC.
52. H. Akaike, Information theory and an extension of the maximum likelihood principle, in *Selected Papers of Hirotugu Akaike* (Springer New York, 1998), pp. 199–213.
53. J. P. Fine, Comparing nonnested cox models. *Biometrika* **89**, 635–648 (2002).
54. T. Hielscher. nonnestcox: Comparing nonnested CoxPH models (2023); https://github.com/thomashielscher/nonnestcox.
55. M. Battaglia, M. S. Anderson, J. H. Buckner, S. M. Geyer, P. A. Gottlieb, T. W. Kay, Å. Lernmark, S. Muller, A. Pugliese, B. O. Roep, C. J. Greenbaum, M. Peakman, Understanding and preventing type 1 diabetes through the unique working model of trialnet. *Diabetologia* **60**, 2139–2147 (2017).
56. M. A. Atkinson, B. O. Roep, A. Posgai, D. C. Wheeler, M. Peakman, The challenge of modulating β-cell autoimmunity in type 1 diabetes. *Lancet Diabetes Endocrinol.* **7**, 52–64 (2019).
57. E. Gülden, N. K. Vudattu, S. Deng, P. Preston-Hurlburt, M. Mamula, J. C. Reed, S. Mohandas, B. C. Herold, R. Torres, S. M. Vieira, B. Lim, J. D. Herazo-Maya, M. Kriegel, A. L. Goodman, C. Cotsapas, K. C. Herold, Microbiota control immune regulation in humanized mice. *JCI Insight* **2**, e91709 (2017).
58. C. Maffeis, A. Martina, M. Corradi, S. Quarella, N. Nori, S. Torriani, M. Plebani, G. Contreas, G. E. Felis, Association between intestinal permeability and faecal microbiota composition in Italian children with β cell autoimmunity at risk for type 1 diabetes. *Diabetes Metab. Res. Rev.* **32**, 700–709 (2016).
59. C. Sorini, I. Cosorich, M. Lo Conte, L. De Giorgi, F. Facciotti, R. Lucianò, M. Rocchi, R. Ferrarese, F. Sanvito, F. Canducci, M. Falcone, Loss of gut barrier integrity triggers activation of islet-reactive T cells and autoimmune diabetes. *Proc. Natl. Acad. Sci. U.S.A. U.S. A.* **116**, 15140–15149 (2019).
60. A. Paun, C. Yau, J. S. Danska, Immune recognition and response to the intestinal microbiome in type 1 diabetes. *J. Autoimmun.* **71**, 10–18 (2016).
61. E. Mariño, J. L. Richards, K. H. McLeod, D. Stanley, Y. A. Yap, J. Knight, C. McKenzie, J. Kranich, A. C. Oliveira, F. J. Rossello, B. Krishnamurthy, C. M. Nefzger, L. Macia, A. Thorburn, A. G. Baxter, G. Morahan, L. H. Wong, J. M. Polo, R. J. Moore, T. J. Lockett, J. M. Clarke, D. L. Topping, L. C. Harrison, C. R. Mackay, Gut microbial metabolites limit the frequency of autoimmune T cells and protect against type 1 diabetes. *Nat. Immunol.* **18**, 552–562 (2017).
62. O. Rouxel, J. D. Silva, L. Beaudoin, I. Nel, C. Tard, L. Cagninacci, B. Kiaf, M. Oshima, M. Diedisheim, M. Salou, A. Corbett, J. Rossjohn, J. M. Cluskey, R. Scharfmann, M. Battaglia, M. Polak, O. Lantz, J. Beltrand, A. Lehuen, Cytotoxic and regulatory roles of mucosal-associated invariant T cells in type 1 diabetes. *Nat. Immunol.* **18**, 1321–1331 (2017).
63. A. M. Gazali, A.-M. Schroderus, K. Näntö-Salonen, R. Rintamäki, J. Pihlajamäki, M. Knip, R. Veijola, J. Toppari, J. Ilonen, T. Kinnunen, Mucosal-associated invariant T cell alterations during the development of human type 1 diabetes. *Diabetologia* **63**, 2396–2409 (2020).
64. C. J. Stewart, N. J. Ajami, J. L. O'Brien, D. S. Hutchinson, D. P. Smith, M. C. Wong, M. C. Ross, R. E. Lloyd, H. V. Doddapaneni, G. A. Metcalf, D. Muzny, R. A. Gibbs, T. Vatanen, C. Huttenhower, R. J. Xavier, M. Rewers, W. Hagopian, J. Toppari, A.-G. Ziegler, J.-X. She, B. Akolkar, A. Lernmark, H. Hyoty, K. Vehik, J. P. Krischer, J. F. Petrosino, Temporal development of the gut microbiome in early childhood from the teddy study. *Nature* **562**, 583–588 (2018).
65. T. Vatanen, E. A. Franzosa, R. Schwager, S. Tripathi, T. D. Arthur, K. Vehik, Å. Lernmark, W. A. Hagopian, M. J. Rewers, J.-X. She, J. Toppari, A.-G. Ziegler, B. Akolkar, J. P. Krischer, C. J. Stewart, N. J. Ajami, J. F. Petrosino, D. Gevers, H. Lähdesmäki, H. Vlamakis, C. Huttenhower, R. J. Xavier, The human gut microbiome in early-onset type 1 diabetes from the teddy study. *Nature* **562**, 589–594 (2018).
66. M. F. Laursen, M. Sakanaka, N. von Burg, U. Mörbe, D. Andersen, J. M. Moll, C. T. Pekmez, A. Rivollier, K. F. Michaelsen, C. Mølgaard, M. V. Lind, L. O. Dragsted, T. Katayama, H. L. Frandsen, A. M. Vinggaard, M. I. Bahl, S. Brix, W. Agace, T. R. Licht, H. M. Roager, Bifidobacterium species associated with breastfeeding produce aromatic lactic acids in the infant gut. *Nat. Microbiol.* **6**, 1367–1382 (2021).
67. T. Vatanen, A. D. Kostic, E. d'Hennezel, H. Siljander, E. A. Franzosa, M. Yassour, R. Kolde, H. Vlamakis, T. D. Arthur, A.-M. Hämäläinen, A. Peet, V. Tillmann, R. Uibo, S. Mokurov, N. Dorshakova, J. Ilonen, S. M. Virtanen, S. J. Szabo, J. A. Porter, H. Lähdesmäki, C. Huttenhower, D. Gevers, T. W. Cullen, M. Knip; DIABIMMUNE Study Group, R. J. Xavier, Variation in microbiome LPS immunogenicity contributes to autoimmunity in humans. *Cell* **165**, 842–853 (2016).
68. A. Are, L. Aronsson, S. Wang, G. Greicius, Y. K. Lee, J.-Å. Gustafsson, S. Pettersson, V. Arulampalam, *Enterococcus faecalis* from newborn babies regulate endogenous PPARγ activity and IL-10 levels in colonic epithelial cells. *Proc. Natl. Acad. Sci. U.S.A.* **105**, 1943–1948 (2008).
69. S. Wang, M. L. Hibberd, S. Pettersson, Y. K. Lee, *Enterococcus faecalis* from healthy infants modulates inflammation through MAPK signaling pathways. *PLOS ONE* **9**, e97523 (2014).
70. N. Steck, M. Hoffmann, I. G. Sava, S. C. Kim, H. Hahne, S. L. Tonkonogy, K. Mair, D. Krueger, M. Pruteanu, F. Shanahan, R. Vogelmann, M. Schemann, B. Kuster, R. B. Sartor, D. Haller, *Enterococcus faecalis* metalloprotease compromises epithelial barrier and contributes to intestinal inflammation. *Gastroenterology* **141**, 959–971 (2011).
71. C. K. Stein-Thoeringer, K. B. Nichols, A. Lazrak, M. D. Docampo, A. E. Slingerland, J. B. Slingerland, A. G. Clurman, G. Armijo, A. L. Gomes, Y. Shono, A. Staffas, M. Burgos da Silva, S. M. Devlin, K. A. Markey, D. Bajic, R. Pinedo, A. Tsakmaklis, E. R. Littmann, A. Pastore, Y. Taur, S. Monette, M. E. Arcila, A. J. Pickard, M. Maloy, R. J. Wright, L. A. Amoretti, E. Fontana, D. Pham, M. A. Jamal, D. Weber, A. D. Sung, D. Hashimoto, C. Scheid, J. B. Xavier, J. A. Messina, K. Romero, M. Lew, A. Bush, L. Bohannon, K. Hayasaka, Y. Hasegawa, M. J. Vehreschild, J. R. Cross, D. M. Ponce, M. A. Perales, S. A. Giralt, R. R. Jenq, T. Teshima, E. Holler, N. J. Chao, E. G. Pamer, J. U. Peled, M. R. van den Brink, Lactose drives *Enterococcus* expansion to promote graft-versus-host disease. *Science* **366**, 1143–1149 (2019).
72. A. Metwaly, S. Reitmeier, D. Haller, Microbiome risk profiles as biomarkers for inflammatory and metabolic disorders. *Nat. Rev. Gastroenterol. Hepatol.* **19**, 383–397 (2022).
73. M. M. Leonard, F. Valitutti, H. Karathia, M. Pujolassos, V. Kenyon, B. Fanelli, J. Troisi, P. Subramanian, S. Camhi, A. Colucci, G. Serena, S. Cucchiara, C. M. Trovato, B. Malamisura, R. Francavilla, L. Elli, N. A. Hasan, A. R. Zomorrodi, R. Colwell, A. Fasano, M. Montuori, P. Piemontese, A. Calvi, M. Baldassarre, L. Norsa, C. L. Raguseo, T. Passaro, P. Roggero, M. Crocco, A. Morelli, M. Perrone, N. Sansotta, M. Chieppa, G. Scala, M. E. Lionetti, C. Catassi, A. Serretiello, C. Vecchi, G. C. de Villsante, Microbiome signatures of progression toward celiac disease onset in at-risk children in a longitudinal prospective cohort study. *Proc. Natl. Acad. Sci. U.S.A.* **118**, e2020322118 (2021).
74. D. A. Schoenfeld, Sample-size formula for the proportional-hazards regression model. *Biometrics* **39**, 499–503 (1983).

75. P. J. Carter, W. S. Cutfield, P. L. Hofman, A. J. Gunn, D. A. Wilson, P. W. Reed, C. Jefferies, Ethnicity and social deprivation independently influence metabolic control in children with type 1 diabetes. *Diabetologia* **51**, 1835–1842 (2008).
76. A. R. Khanolkar, R. Amin, D. Taylor-Robinson, R. M. Viner, J. T. Warner, T. Stephenson, Young people with type 1 diabetes of non-white ethnicity and lower socio-economic status have poorer glycaemic control in England and Wales. *Diabet. Med.* **33**, 1508–1515 (2016).
77. A. R. Khanolkar, R. Amin, D. Taylor-Robinson, R. M. Viner, J. Warner, E. F. Gevers, T. Stephenson, Ethnic differences in early glycemic control in childhood-onset type 1 diabetes. *BMJ Open Diabetes Res. Care* **5**, e000423 (2017).
78. R. B. Lipton, M. Drum, S. A. Greeley, K. K. Danielson, G. I. Bell, W. A. Hagopian, HLA-DQ haplotypes differ by ethnicity in patients with childhood-onset diabetes. *Pediatr. Diabetes* **12**Pt. 2, 388–395 (2011).
79. J. A. Noble, J. Johnson, J. A. Lane, A. M. Valdes, HLA class II genotyping of African American type 1 diabetic patients reveals associations unique to African haplotypes. *Diabetes* **62**, 3292–3299 (2013).
80. S. Onengut-Gumuscu, W.-M. Chen, C. C. Robertson, J. K. Bonnie, E. Farber, Z. Zhu, J. R. Oksenberg, S. R. Brant, S. L. Bridges, J. C. Edberg, R. P. Kimberly, P. K. Gregersen, M. J. Rewers, A. K. Steck, M. H. Black, D. Dabelea, C. Pihoker, M. A. Atkinson, L. E. Wagenknecht, J. Divers, R. A. Bell; SEARCH for Diabetes in Youth; Type 1 Diabetes Genetics Consortium, H. A. Erlich, P. Concannon, S. S. Rich, Type 1 diabetes risk in African-ancestry participants and utility of an ancestry-specific genetic risk score. *Diabetes Care* **42**, 406–415 (2019).
81. W. Woo, J. M. LaGasse, Z. Zhou, R. Patel, J. P. Palmer, H. Campus, W. A. Hagopian, A novel high-throughput method for accurate, rapid, and economical measurement of multiple type 1 diabetes autoantibodies. *J. Immunol. Methods* **244**, 91–103 (2000).
82. J. M. Wenzlau, K. Juhl, L. Yu, O. Moua, S. A. Sarkar, P. Gottlieb, M. Rewers, G. S. Eisenbarth, J. Jensen, H. W. Davidson, J. C. Hutton, The cation efflux transporter znt8 (slc30a8) is a major autoantigen in human type 1 diabetes. *Proc. Natl. Acad. Sci. U.S.A.* **104**, 17040–17045 (2007).
83. R Core Team, *R: A Language and Environment for Statistical Computing* (R Foundation for Statistical Computing, 2019); www.R-project.org/.
84. D. R. Nyholt, A simple correction for multiple testing for single-nucleotide polymorphisms in linkage disequilibrium with each other. *Am. J. Hum. Genet.* **74**, 765–769 (2004).
85. T. Therneau, A package for survival analysis in R (2022); https://CRAN.R-project.org/package=survival.
86. J. Fox, S. Weisberg, *An R Companion to Applied Regression* (Sage, ed. 3, 2019); https://socialsciences.mcmaster.ca/jfox/Books/Companion/.
87. T. M. Therneau, P. M. Grambsch, *Modeling Survival Data: Extending the Cox Model* (Springer, 2000).
88. I. Letunic, P. Bork, Interactive tree of life (itol) V5: An online tool for phylogenetic tree display and annotation. *Nucleic Acids Res.* **49**, W293–W296 (2021).
89. E. Henderson, ghibli: Studio Ghibli colour palettes (2022); https://CRAN.R-project.org/package=ghibli.
90. R. Boyes, Forester: An R package for creating publication-ready forest plots (2021); https://github.com/rdboyes/forester.

Acknowledgments: We thank the TrialNet Steering and Manuscript committees for their collegiality and interest in the work. We also thank the participants and clinical care providers of the TN-10 study for their essential contributions to this work. **Funding:** This work was supported by grants from Canadian Institutes of Health Research (CIHR) 363923 (to J.S.D.), CIHR and JDRF (joint-funded grant) 168480 (to J.S.D.), JDRF SRA-2019-833-S-B (to K.C.H. and J.S.D.), NIH R01 DK057846 (to K.C.H.), Anne and Max Tanenbaum Chair in Molecular Medicine (to J.S.D.), and the Hospital for Sick Children Foundation (to J.S.D.). The teplizumab study was funded by the Type 1 Diabetes TrialNet Study Group, which is a clinical trials network funded through a cooperative agreement by the National Institutes of Health (NIH) through the National Institute of Diabetes and Digestive and Kidney Diseases (NIDDK), the National Institute of Allergy and Infectious Diseases (NIAID), the Eunice Kennedy Shriver National Institute of Child Health and Human Development, and JDRF. **Author contributions:** Q.Y.X., K.C.H., and J.S.D. conceptualized the study. Q.Y.X., S.O., A.W., C.Y., and J.S.D. developed the methodology, and Q.Y.X., S.O., A.W., and C.Y. performed the experimental studies. Q.Y.X., A.W., and C.Y. analyzed the data. Q.Y.X. and J.S.D. wrote the manuscript. Q.Y.X., C.Y., K.C.H., and J.S.D. reviewed and edited the manuscript. **Competing interests:** K.C.H. is a coinventor on patents US-20230013752-A1, "Methods for delaying onset of type 1 diabetes"; US-11434291-B2, "Methods and compositions for preventing type 1 diabetes"; and US-20220041720-A1 and US-20200399368-A1, "Methods and compositions for preventing type 1 diabetes" but has no financial interests. The other authors declare that they have no competing interests. **Data and materials availability:** The code for analyses is available at DOI: 10.5281/zenodo.8378069. The primary data used to generate graphs are provided in data file S1. The metadata of TN-10 participants are available upon request from the TrialNet data coordinating center.

Submitted 6 February 2023
Resubmitted 04 July 2023
Accepted 2 October 2023
Published 25 October 2023
10.1126/scitranslmed.adh0353

Science Translational Medicine

Immune responses to gut bacteria associated with time to diagnosis and clinical response to T cell–directed therapy for type 1 diabetes prevention

Quin Yuhui Xie, Sean Oh, Anthony Wong, Christopher Yau, Kevan C. Herold, and Jayne S. Danska

Sci. Transl. Med. **15** (719), eadh0353. DOI: 10.1126/scitranslmed.adh0353